SINE–GORDON SOLITONS, KINKS AND BREATHERS AS PHYSICAL MODELS OF NONLINEAR EXCITATIONS IN LIVING CELLULAR STRUCTURES

VLADIMIR G. IVANCEVIC AND TIJANA T. IVANCEVIC

Communicated by Ivaïlo M. Mladenov

Abstract.   Nonlinear space-time dynamics, defined in terms of celebrated 'solitonic' equations, brings indispensable tools for understanding, prediction and control of complex behaviors in both physical and life sciences. In this paper, we review sine–Gordon solitons, kinks and breathers as models of nonlinear excitations in complex systems in physics and in living cellular structures, both intra–cellular (DNA, protein folding and microtubules) and inter–cellular (neural impulses and muscular contractions).

Contents

1. Introduction

In spatiotemporal dynamics of complex nonlinear systems (see [53, 55, 58, 60]), Sine–Gordon equation (SGE) is, together with Korteweg–deVries (KdV) and non-linear Schrödinger (NLS) equations, one of the celebrated nonlinear-yet-integrable partial differential equations (PDEs), with a variety of traveling solitary waves as solutions (see Fig. 1 and Fig. 2, as well as the following basic references [3, 11, 26, 82, 83, 88, 91]). For a soft SGE–intro, see the popular web-sites [106, 107]. From rigorous geometrical perspective, both KdV and NLS equations are mentioned in Subsection 3.5 below as solitary models for muscular contractions on Poisson manifolds.

Briefly, a solitary wave is a traveling wave (with velocity v) of the form $\phi(x, t) = f(x - vt)$, for a smooth function f that decays rapidly at infinity e.g. a nonlinear wave equation $\phi_{tt} - \phi_{xx} = \phi(2\phi^2 - 1)$ has a family of solitary–wave solutions $\phi(x, t) = \text{sech}(x\cosh\mu + t\sinh\mu)$, parameterized by $\mu \in \mathbb{R}$ (see [105]). In complex physical systems, SGE solitons, kinks and breathers appear in various situations, including propagation of magnetic flux (fluxons) in long Josephson junctions [10, 68], dislocations in crystals [9, 33], nonlinear spin waves in superfluids [68], and waves in ferromagnetic and anti-ferromagnetic materials [114, 115] – to mention just a few application areas.

In this paper, we review physical theory of sine–Gordon solitons, kinks and breathers, as well as their essential dynamics of nonlinear excitations in living cellular structures, both intra–cellular (DNA, protein folding and microtubules) and inter–cellular (neural impulses and muscular contractions).

We show that sine–Gordon traveling waves can give us new insights even in such long–time established and Nobel–Prize winning living systems as the Watson–Crick double helix DNA model and the Hodgkin–Huxley neural conduction model.
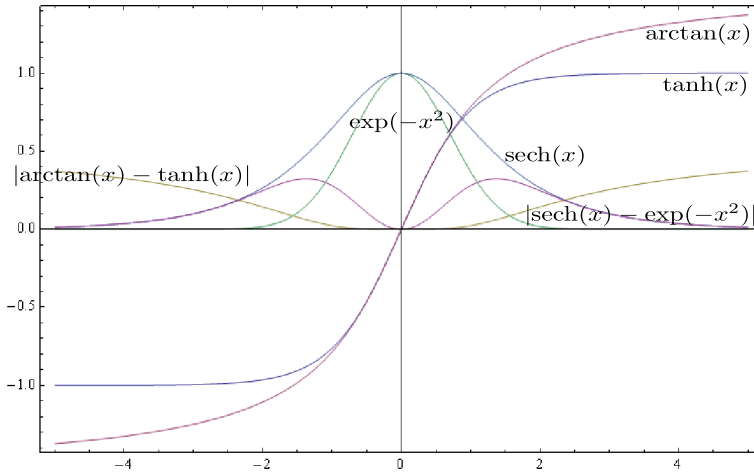
Figure 1. Basic static examples of kinks $\tanh(x)$, $\arctan(x)$ and bell–shaped solitons $\text{sech}(x)$, $\exp(-x^2)$, together with their (absolute) differences; plotted in `Mathematica`®.

2. Physical Theory of Sine–Gordon Solitons, Kinks and Breathers

In this section, we give the basic theory of the sine–Gordon equation (and the variety of its traveling–wave solutions), as spatiotemporal models of nonlinear excitations in complex physical systems.

2.1. Sine–Gordon Equation (SGE)

SGE is a real-valued, hyperbolic, nonlinear wave equation defined on $\mathbb{R}^{1,1}$, which appears in two equivalent forms (using standard indicial notation for partial derivatives $\phi_{zz} = \partial_z^2 \phi = \partial^2 \phi / \partial z^2$)

- In the (1+1) space-time $(x, t)-$coordinates, the SGE reads

$$\phi_{tt} = \phi_{xx} - \sin\phi \qquad \text{or} \qquad \phi_{tt}(x,t) = \phi_{xx}(x,t) - \sin\phi(x,t) \qquad (1)$$

which shows that it is a nonlinear extension of the standard linear wave equation $\phi_{tt} = \phi_{xx}$. The solutions $\phi(x,t)$ of (1) determine the internal Riemannian geometry of surfaces of constant negative scalar curvature $R = -2$, given by the line-element

$$ds^2 = \sin^2\left(\frac{\phi}{2}\right) dt^2 + \cos^2\left(\frac{\phi}{2}\right) dx^2$$

where the angle ϕ describes the embedding of the surface into Euclidean space $\mathbb{R}^3$ (see [11]). A basic solution of the SGE (1) is

$$\phi(x,t) = 4 \arctan\left[\exp\left(\pm\frac{x-vt}{\sqrt{1-v^2}}\right)\right] \tag{2}$$

describing a *soliton* moving with velocity $0 \leq v < 1$ and changing the phase from 0 to 2π (*kink,* the case of $+$ sign) or from 2π to 0 (*anti-kink,* the case of $-$ sign). Each traveling soliton solution of the SGE has the corresponding surface in $\mathbb{R}^3$ (see [105]).

- In the (1+1) light-cone $(u,v)-$coordinates, defined by $u = (x+t)/2$, $v = (x+t)/2$, in which the line-element (depending on the angle ϕ between two asymptotic lines $u = \text{const}, v = \text{const}$) is given by

$$\mathrm{d}s^2 = \mathrm{d}u^2 + 2\cos\phi\,\mathrm{d}u\,\mathrm{d}v + \mathrm{d}v^2$$

the SGE describes a family of pseudo-spherical surfaces with constant Gaussian curvature $K = -1$, and reads

$$\phi_{uv} = \sin\phi \qquad \text{or} \qquad \phi_{uv}(u,v) = \sin\phi(u,v). \tag{3}$$

SGE (3) is the single Codazzi–Mainardi compatibility equation between the first (I_G) and second (II_C) fundamental forms of a surface, defined by the Gauss and Codazzi equations, respectively

$$I_\mathrm{G} = \mathrm{d}u^2 + 2\cos\phi\,\mathrm{d}u\,\mathrm{d}v + \mathrm{d}v^2 \qquad \text{and} \qquad II_\mathrm{C} = 2\sin\phi\,\mathrm{d}u\,\mathrm{d}v.$$

A typical, spatially-symmetric, boundary-value problem for (1) is defined by

$$x \in [-L, L] \subset \mathbb{R}, \qquad t \in \mathbb{R}^+ \qquad \text{with}$$
$$\phi(x,0) = f(x), \qquad \phi_t(x,0) = 0, \qquad \phi(-L,t) = \phi(L,t)$$

where $f(x) \in \mathbb{R}$ is an axially-symmetric function (e.g. Gaussian or sech, see Fig. 3).

Bäcklund Transformations (BT) for the SGE (1) were devised in 1880s in Riemannian geometry of surfaces and are attributed to Bianchi and Bäcklund. In 1883, A. Bäcklund showed that if $L : M \to M'$ is a pseudo-spherical line congruence between two surfaces M, M', then both M and M' are pseudo-spherical and L maps asymptotic lines on M to asymptotic lines on M'. Analytically, this is equivalent
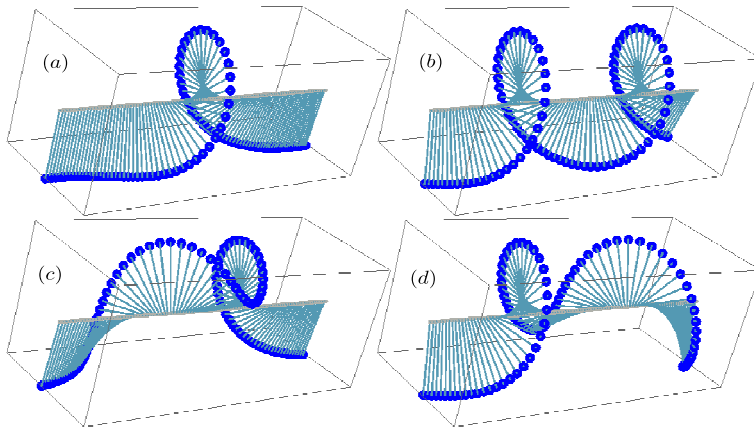
Figure 2. Basic solitary SGE–solutions, simulated in `Mathematica`® as systems of spring-coupled torsional pendula: (a) single soliton $\phi(x,t)=4\arctan\left(\exp\frac{x-vt}{1-v^2}\right)$, (b) soliton–soliton collision $\phi(x,t)=4\arctan\left(\frac{v\sinh\frac{x}{1-v^2}}{\cosh\frac{vt}{1-v^2}}\right)$, (c) soliton–antisoliton collision $\phi(x,t)=4\arctan\left(\frac{\sinh\frac{vt}{1-v^2}}{v\cosh\frac{x}{1-v^2}}\right)$, and (d) single breather $\phi(x,t)=4\arctan\left(\frac{\sin\frac{vt}{1-v^2}}{v\cosh\frac{x}{1-v^2}}\right)$ (modified and adapted from [80]).

to the statement that if ϕ is a solution of the SGE (1), then so are also the solutions of the ODE system (4) (see, e.g. [14]).

BT have the form

$$\frac{1}{2}(\phi+\varphi)_\xi = \alpha\sin\frac{\phi-\varphi}{2}, \qquad \frac{1}{2}(\phi-\varphi)_\eta = \frac{1}{\alpha}\sin\frac{\phi+\varphi}{2} \qquad (4)$$

where both ϕ and φ are solutions of the SGE (1), and can be viewed as a transformation of the SGE into itself. BT (4) allows one to find a two-parameter family of solutions, given a particular solution ϕ_0 of (1). For example, consider the trivial solution $\phi = 0$ that, substituted into (4), gives

$$\varphi_\xi = -2\alpha\sin\frac{\varphi}{2}, \qquad \varphi_\eta = -\frac{2}{\alpha}\sin\frac{\varphi}{2}$$

which, by integration, gives

$$2\alpha\xi = -2\ln(\tan\frac{\varphi}{4}) + p(\eta), \qquad \frac{2}{\alpha}\eta = -2\ln(\tan\frac{\varphi}{4}) + p(\xi)$$

from which the following new solution is generated

$$\varphi = 4\arctan\left[\exp(-\alpha\xi - \frac{1}{\alpha}\eta + \text{const})\right].$$
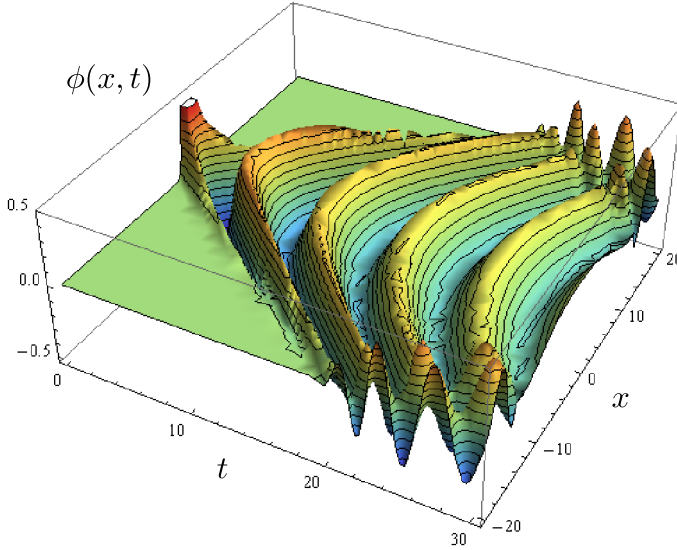
Figure 3. Numerical solution of the SGE (1) in `Mathematica`® , using numerical ODE/PDE integrator NDSolve, with the following data (including the Gaussian initial state, zero initial velocity and symmetric boundary condition) $x \in [-20, 20]$, $t \in [0, 30]$, $\phi(x, 0) = \exp(-x^2)$, $\phi_t(x, 0) = 0$, $\phi(-20, t) = \phi(20, t)$. The waves oscillate around the zero plane and increase their width with time. Both near-periodicity and nonlinearity of the time evolution are apparent.

The sine–forcing term in the SGE can be viewed as a *nonlinear deformation* $\phi \to \sin \phi$, of the linear forcing term in the Klein–Gordon equation (KGE, a vacuum linearization of the SGE), which is commonly used for describing scalar fields in (quantum) field theory

$$\phi_{tt} = \phi_{xx} - \phi. \tag{5}$$

This, in turn, implies that (as a field equation) SGE can be derived as an Euler–Lagrangian equation from the Lagrangian density

$$\mathcal{L}_{\text{SG}}(\phi) = \frac{1}{2}(\phi_t^2 - \phi_x^2) - 1 + \cos \phi. \tag{6}$$

It could be expected that $\mathcal{L}_{\text{SG}}(\phi)$ is a 'deformation' of the KG Lagrangian

$$\mathcal{L}_{\text{KG}}(\phi) = \frac{1}{2}(\phi_t^2 - \phi_x^2) - \frac{\phi^2}{2}. \tag{7}$$

That can be demonstrated by the Taylor–series expansion of the cosine term

$$\cos \phi = \sum_{n=0}^{\infty} \frac{(-\phi^2)^n}{(2n)!}$$

so that we have the following relationship between the two Lagrangians

$$\mathcal{L}_{\text{SG}}(\phi) = \mathcal{L}_{\text{KG}}(\phi) + \sum_{n=2}^{\infty} \frac{(-\phi^2)^n}{(2n)!}.$$
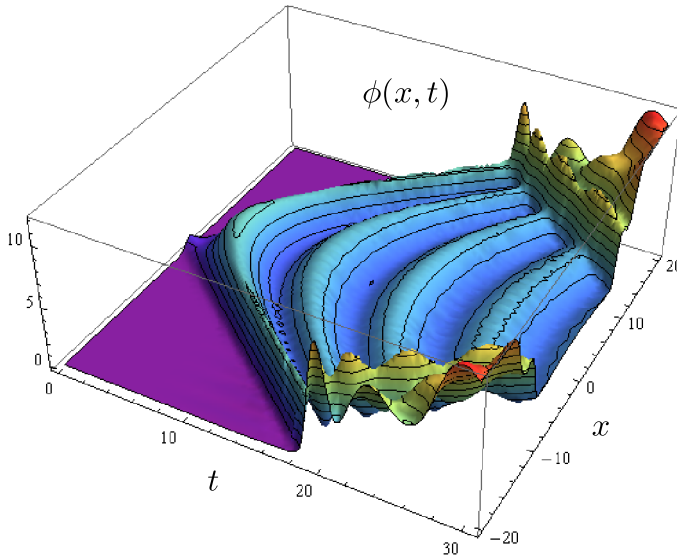
Figure 4. Numerical solution of the SGE (17) in `Mathematica`® , with the following data (including the Gaussian initial state, zero initial velocity and symmetric boundary condition) $x \in [-20, 20]$, $t \in [0, 30]$, $\phi(x, 0) = \exp(-x^2)$, $\phi_t(x, 0) = 0$, $\phi(-20, t) = \phi(20, t)$. Under the same boundary conditions, the SGE with the plus sine gives about 20 times higher amplitude waves, which are all above the zero plane and decrease their width with time. Again, both near-periodicity and nonlinearity of the time evolution are apparent.

The corresponding Hamiltonian densities, of kinetic plus potential energy type, are given in terms of canonically–conjugated coordinate and momentum fields by

$$\mathcal{H}_{\text{SG}}(\phi, \pi) = \pi\phi_t - \mathcal{L}_{\text{SG}}(\phi) = \frac{1}{2}(\pi^2 + \phi_x^2) + 1 - \cos\phi$$

$$\mathcal{H}_{\text{KG}}(\phi, \pi) = \pi\phi_t - \mathcal{L}_{\text{KG}}(\phi) = \frac{1}{2}(\pi^2 + \phi_x^2) + \phi^2.$$

Both SGE and KGE are infinite–dimensional Hamiltonian systems [104], with Poisson brackets given by

$$\{F, G\} = \int_{-\infty}^{\infty} \left[\frac{\delta F}{\delta \phi(x)} \frac{\delta G}{\delta \pi(x)} - \frac{\delta F}{\delta \pi(x)} \frac{\delta G}{\delta \phi(x)} \right] \mathrm{d}x \tag{8}$$

so that both (1) and (5) follow from Hamilton's equations with Hamiltonian H and symplectic form ω

$$\phi_t = \{H, \phi\}, \qquad \pi_t = \{H, \pi\} \qquad \text{with}$$
$$H = \int_{-\infty}^{\infty} \mathcal{H}(\phi, \pi) \, \mathrm{d}x, \qquad \omega = \int_{-\infty}^{\infty} (\mathrm{d}\pi \wedge \mathrm{d}\phi) \, \mathrm{d}x. \tag{9}$$

The Hamiltonian (9) is conserved by the flow of both SGE (1) and KGE (5), with an infinite number of commuting constants of motion (common level sets of these constants of motion are generically infinite-dimensional tori of maximal dimension). Both SGE and KGE admit their own infinite families of conserved functionals in involution with respect to their Poisson bracket (8). This fact allows them both to be solved with the *inverse scattering transform* (see [26]). For the Poisson–manifold generalization, see Section 3.5 below.

2.2. Momentum and Energy of SGE Solitons

SGE is Lorentz–covariant, i.e., invariant with respect to special–relativistic Lorentz transformations. Each SGE–soliton behaves as a relativistic object and contracts when $v \to c \equiv$ the speed of light, and for this fact it has been used in (quantum) field theory.

In both forms (1) and (3), the SGE has the following symmetries

$t \to t + t_0,$	$x \to x,$	$\phi \to \phi$	(shift in t)
$t \to t,$	$x \to x + x_0,$	$\phi \to \phi$	(shift in x)
$t \to t,$	$x \to x,$	$\phi \to \phi + 2\pi n$	(discrete shifts in ϕ)
$t \to -t,$	$x \to x,$	$\phi \to \phi$	(reflection in t)
$t \to t,$	$x \to -x,$	$\phi \to \phi$	(reflection in x)
$t \to t,$	$x \to x,$	$\phi \to -\phi$	(reflection in ϕ)
$t \to \dfrac{t - vx}{\sqrt{1 - v^2}},$	$x \to \dfrac{x - vx}{\sqrt{1 - v^2}},$	$\phi \to \phi$	(Lorentz boost)

where e.g. reflection in ϕ means if ϕ is a solution then so is $-\phi$, etc.

In Minkowski (1+1) space-time coordinates ($x^\mu \in \mathbb{R}^{1,1}$, $x^0 = t$, $x^1 = x$) with metric tensor $\eta_{\mu\nu}$ ($\mu, \nu = 0, 1, \eta_{11} = -\eta_{22} = 1, \eta_{11} = \eta_{11} = 0$), the SG–Lagrangian density has the following 'massive form' of kinetic minus potential energy, with mass m and coupling constant λ (see [91])

$$\mathcal{L}_{SG}^{Mink}(\phi) = \frac{1}{2}(\phi_t^2 - \phi_x^2) - \frac{m^4}{\lambda}\left[1 - \cos(\frac{\sqrt{\lambda}}{m}\phi)\right]$$

which reduces to the dimensionless form (6) by re-scaling the fields and coordinates

$$\frac{\sqrt{\lambda}}{m}\phi \to \phi, \qquad mx^\mu \to x^\mu. \tag{10}$$

The SG–Lagrangian density $\mathcal{L}_{SG}^{Mink}(\phi) \equiv \frac{m^4}{\lambda}\mathcal{L}_{SG}(\phi)$ obeys the conservation law and admits topological (i.e., not sensitive to local degrees of freedom) *Noether current* with respect to (10)

$$j^\mu = \frac{1}{2\pi}\varepsilon^{\mu\nu}\partial_\nu\phi \quad \text{with zero-divergence} \quad \partial_\mu j^\mu = 0$$

where $\varepsilon^{\mu\nu}$ is the $\mathbb{R}^{1,1}$–Levi–Civita tensor. The corresponding topological *Noether charge* is given by

$$Q = \int \left|\partial_t j^0(x,t)\right| \mathrm{d}x = \frac{1}{2\pi}\left|\phi(+\infty,t) - \phi(-\infty,t)\right|$$

with

$$Q_t = \frac{1}{2\pi}\left|\phi_t(-\infty,t) - \phi_t(+\infty,t)\right| = 0.$$

The most important physical quality of the SGE is its energy–momentum (EM) tensor $T_{\mu\nu}$, which is the Noether current corresponding to spacetime–translation symmetry $x^\mu \to x^\mu + \xi^\mu$ and this conserved quantity is derived from the Lagrangian (6) as

$$T_{\mu\nu} = \partial_\mu\phi\partial_\nu\phi - \eta_{\mu\nu}\mathcal{L}_{SG}(\phi).$$

The energy-momentum $T_{\mu\nu}$ has the following components [39, 91]

$$T_{00} = \frac{1}{2}(\phi_t^2 + \phi_x^2) + 1 - \cos\phi, \qquad T_{10} = \phi_{xt} = T_{01}$$

$$T_{11} = \frac{1}{2}(\phi_t^2 + \phi_x^2) - 1 + \cos\phi.$$

EM's contravariant tensor $T^{\mu\nu}$ has the following components

$$T^{00} = T_{00}, \qquad T^{11} = T_{11}, \qquad T^{10} = -T_{01}$$

obtained by raising the indices of $T_{\mu\nu}$ using the inverse metric tensor $\eta^{\mu\nu} = 1/(\eta)_{\mu\nu}$.

EM's conserved quantities are *momentum* $P = \int T^{10}\mathrm{d}x$, which is the Noether charge with respect to space–translation symmetry, and *energy* $E = \int T^{00}\mathrm{d}x$, which is the Noether charge with respect to time–translation symmetry. Energy and momentum follow from EM's zero divergence

$$\partial_\mu T^{\mu\nu} = 0 \implies \begin{cases} \partial_t T^{00} - \partial_x T^{10} = 0 \\ \partial_t T^{01} - \partial_x T^{11} = 0 \end{cases} \implies \begin{cases} \partial_t E = \partial_t \int T^{00}\mathrm{d}x = 0 \\ \partial_t P = \partial_t \int T^{10}\mathrm{d}x = 0. \end{cases}$$

2.3. SGE Solutions and Integrability

2.3.1. SGE Solitons, Kinks and Breathers

The first *1-soliton* solution of the SGE (1) was given by [2, 4] in the form

$$\phi(x,t) = 4\arctan\left[\frac{\sqrt{1-\omega^2}\cos(\omega t)}{\omega\cosh(x\sqrt{1-\omega^2})}\right]$$

which, for $\omega < 1$, is periodic in time t and decays exponentially when moving away from $x = 0$.

There is a well-known traveling solitary wave solution with velocity v (see [102]), given by the following generalization of (2)

$$\phi(x,t) = 4\arctan\left[\exp\frac{\pm 2(z-z_0)}{\sqrt{1-v^2}}\right], \qquad \text{with } z = \mu(x+vt) \qquad (11)$$

and the center at z_0. In (11), the case $+2$ describes kink, while the case -2 corresponds to antikink.

The *stationary kink* with the center at x_0 is defined by

$$\phi(x) = 2\arctan\left[\exp(x-x_0)\right]$$

(in which the position of the center x_0 can be varied continuously $-\infty < x_0 < \infty$) and represents the solution of the first-order ODE $\phi_x(x) = \sin\phi(x)$.

Regarding solutions of the slightly more general, three-parameter SGE

$$\phi_{tt} = a\phi_{xx} + b\sin(\lambda\phi) \qquad (12)$$

the following cases were established in the literature (see [88] and references therein)

1. If a function $w = \phi(x,t)$ is a solution of (12), then so are also the following functions

$$w_1 = \frac{2\pi n}{b} \pm \phi(C_1 \pm x, C_2 \pm t) \qquad \text{for} \qquad n = 0, \pm 1, \pm 2, ...$$

$$w_2 = \pm \phi\left(x \cosh C_3 + t\sqrt{a}\sinh C_3, \; x\frac{\sinh C_3}{\sqrt{a}} + t\cosh C_3\right)$$

where C_1, C_2, and C_3 are arbitrary constants.

2. Traveling-wave solutions

$$\phi(x,t) = \frac{4}{\lambda}\arctan\left[\exp\left(\pm\frac{b\lambda(C_1 x + C_2 t + C_3)}{\sqrt{b\lambda(C_2^2 - aC_1^2)}}\right)\right] \qquad (13)$$

if $b\lambda(C_2^2 - aC_1^2) > 0$

$$\phi(x,t) = -\frac{\pi}{\lambda} + \frac{4}{\lambda}\arctan\left[\exp\left(\pm\frac{b\lambda(C_1 x + C_2 t + C_3)}{\sqrt{b\lambda(aC_1^2 - C_2^2)}}\right)\right]$$

if $b\lambda(C_2^2 - aC_1^2) < 0$

where the first expression (for $b\lambda(C_2^2 - aC_1^2) > 0$) represents another one-soliton solution, which is kink in case of $\exp\left(\frac{b\lambda(C_1 x + C_2 t + C_3)}{\sqrt{b\lambda(C_2^2 - aC_1^2)}}\right)$ and antikink in case of $\exp\left(-\frac{b\lambda(C_1 x + C_2 t + C_3)}{\sqrt{b\lambda(C_2^2 - aC_1^2)}}\right)$. In case of the standard SGE (1), this kink–antikink expression specializes to the Lorentz-invariant solution similar to (11)

$$\phi^{\text{K}}(x,t) = 4\arctan\left[\exp\left(\frac{\pm(x - x_c) - vt}{\sqrt{1 - v^2}}\right)\right] \qquad (14)$$

where the velocity v $(0 < v < 1)$ and the soliton-center x_c are real-valued constants. The kink solution has the following physical (EM) characteristics

i) Energy

$$E[\phi^{\text{K}}(x,t)] = \int T^{00}\mathrm{d}x = \frac{8}{\sqrt{1 - v^2}} \qquad \text{and}$$

ii) Momentum

$$P[\phi^{\text{K}}(x,t)] = \int T^{10}\mathrm{d}x = -\frac{8v}{\sqrt{1 - v^2}} \, .$$

3. Functional separable solution

$$w(x,t) = \frac{4}{\lambda} \arctan \left[f(x)g(t) \right]$$

where the functions $f = f(x)$ and $g = g(t)$ are determined by the first-order autonomous separable ODEs

$$f_x^2 = Af^4 + Bf^2 + C, \qquad g_t^2 = -aCg^4 + (aB + b\lambda)g^2 - aA$$

where A, B, and C are arbitrary constants. In particular, for $A = 0, B = k^2 > 0$, and $C > 0$, we have the *two-soliton* solution [87]

$$w(x,t) = \frac{4}{\lambda} \arctan \left[\frac{\eta \sin(kx + A_1)}{k\sqrt{a}\cosh(\eta t + B_1)} \right], \qquad \eta^2 = ak^2 + b\lambda > 0$$

where k, A_1, and B_1 are arbitrary constants.

The only stable traveling wave SGE-solutions for a scalar field ϕ are 2π-kinks [16, 85] (localized solutions with identical boundary conditions $\phi = 0$ and $\phi = 2\pi$). However, easier to follow experimentally are non-localized π-kinks [67] (separating regions with different values of the field ϕ), see also [114] and references therein.

On the other hand, a *breather* is spatially localized, time periodic, oscillatory SGE–solution (see, e.g. [45]). It represents a field which is periodically oscillating in time and decays exponentially in space as the distance from the center $x = 0$ is increased. This oscillatory solution of (1) is characterized by some phase that depends on the breather's evolution history. This could be, in particular, a bound state of vortex with an antivortex in a Josephson junction. In this case, breather may appear as a result of collision of a *fluxon* (a propagating magnetic flux-quantum) with an *antifluxon*, or even in the process of measurements of switching current characteristics. Stationary breather solutions form one-parameter families of solutions. An example of a breather–solution of (1) is given by [40]

$$\phi = 4 \arctan \left(\frac{\sin T}{u \cosh \left(g(u)x \right)} \right)$$

with parameters $u = u(t)$ and $T = T(t)$, such that

$$g(u) = 1/\sqrt{1 + u^2} \quad \text{and} \quad T(t) = \int_0^t g(u(t')) \, u(t') \, \mathrm{d}t'.$$
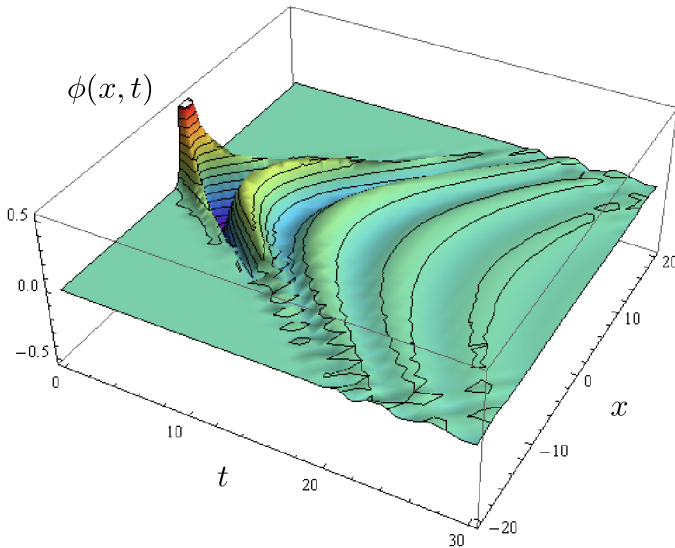
Figure 5.   Numerical solution of the damped, unforced SGE (18) in `Mathematica®` , with the following data (including the Gaussian initial state, zero initial velocity and symmetric boundary condition) $x \in [-20, 20]$, $t \in [0, 30]$, $\phi(x, 0) = \exp(-x^2)$, $\phi_t(x, 0) = 0$, $\phi(-20, t) = \phi(20, t)$, $\gamma = 0.2$, $F(x, t) = 0$. Damping of the waves is apparent.

2.3.2. Lax–Pair and General SGE Integrability

In both cases (1) and (3), the SGE admits a *Lax–pair* formulation

$$\dot{L} = [L, M] \tag{15}$$

where overdot means time derivative, L and M are linear differential operators and $[L, M] \equiv LM - ML$ is their commutator (Lie bracket).

Historically, the first Lax-pair for a nonlinear PDE was found by P. Lax in 1968 consisting of the following two operators [71]

$$L = \frac{\mathrm{d}^2}{\mathrm{d}x^2} - u, \qquad M = 4\frac{\mathrm{d}^3}{\mathrm{d}x^3} - 6u\frac{\mathrm{d}}{\mathrm{d}x} - 3u_x$$

such that their Lax formulation (15) gives the KdV equation

$$u_t - 6uu_x + u_{xxx} = 0 \qquad \text{by}$$

$$L_t = -u_t, \quad LM - ML = u_{xxx} - 6uu_x\,.$$

The Lax-pair form of the KdV–PDE immediately shows that the eigenvalues of L are independent of t. The key importance of Lax's observation is that any PDE

that can be cast into such a framework for other operators L and M, automatically obtains many of the features of the KdV–PDE, including an infinite number of local conservation laws.
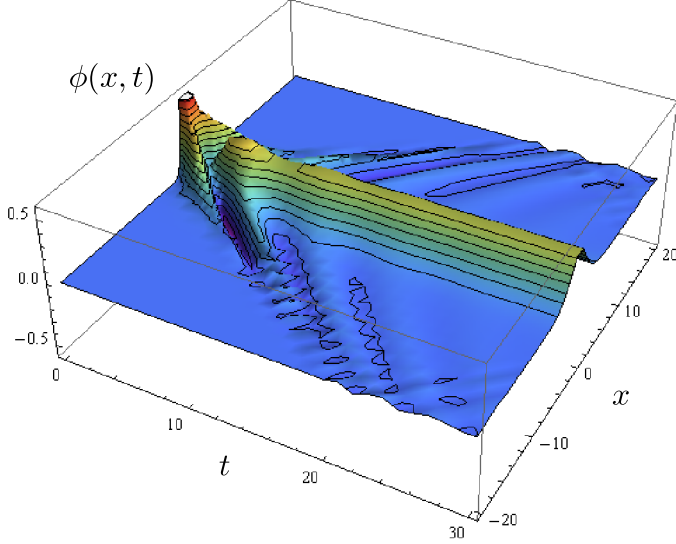
Figure 6. Numerical solution of the damped and spatially-forced SGE (18) in Mathematica® , with the following data (including the Gaussian initial state, zero initial velocity and symmetric boundary condition) $x \in [-20, 20]$, $t \in [0, 30]$, $\phi(x, 0) = \exp(-x^2)$, $\phi_t(x, 0) = 0$, $\phi(-20, t) = \phi(20, t)$, $\gamma = 0.2$, $F(x) = 0.5\mathrm{sech}(x)$. We can see the central sech-forcing along all time axis. Damping of the SG-waves is also apparent.

For example, it was shown in [74] that the SGE (1) is integrable through the following Lax pair

$$\phi_t = L\phi, \qquad \phi_x = M\phi, \qquad \text{where} \qquad (16)$$

$$L = \begin{pmatrix} \frac{\mathrm{i}}{4}(\phi_x + \phi_t) & -\frac{1}{16\lambda}\mathrm{e}^{\mathrm{i}\phi} + \lambda \\ \frac{1}{16\lambda}\mathrm{e}^{-\mathrm{i}\phi} - \lambda & -\frac{\mathrm{i}}{4}(\phi_x + \phi_t) \end{pmatrix}, \qquad \mathrm{i} = \sqrt{-1}$$

$$M = \begin{pmatrix} \frac{\mathrm{i}}{4}(\phi_x + \phi_t) & \frac{1}{16\lambda}\mathrm{e}^{\mathrm{i}\phi} + \lambda \\ -\frac{1}{16\lambda}\mathrm{e}^{-\mathrm{i}\phi} - \lambda & -\frac{\mathrm{i}}{4}(\phi_x + \phi_t) \end{pmatrix}, \qquad \lambda \in \mathbb{R}.$$

The Lax pair (16) possesses the following complex-conjugate symmetry if $\phi = \begin{pmatrix} \phi_1 \\ \phi_2 \end{pmatrix}$ solves the Lax pair (16) at (λ, ϕ), then $\begin{pmatrix} \overline{\phi_2} \\ \overline{\phi_1} \end{pmatrix}$ solves the Lax pair (16) at

$(-\bar{\lambda}, \phi)$. In addition, there is a Darboux transformation for the Lax pair (16) as follows, let

$$u = \phi + 2\mathrm{i}\ln\left[\frac{\mathrm{i}\phi_2}{\phi_1}\right], \qquad u \in \mathbb{R}.$$

If $\phi = \phi|_{\lambda=\nu}$ for some $\nu \in \mathbb{R}$, then

$$\psi = \begin{pmatrix} -\nu\phi_2/\phi_1 & \lambda \\ -\lambda & \nu\phi_1/\phi_2 \end{pmatrix}\phi$$

solves the Lax pair (16) at (λ, u). Also, from its spatial part $\phi_x = M\phi$, a complete Floquet theory can be developed. See [74] for the proofs and more technical details.
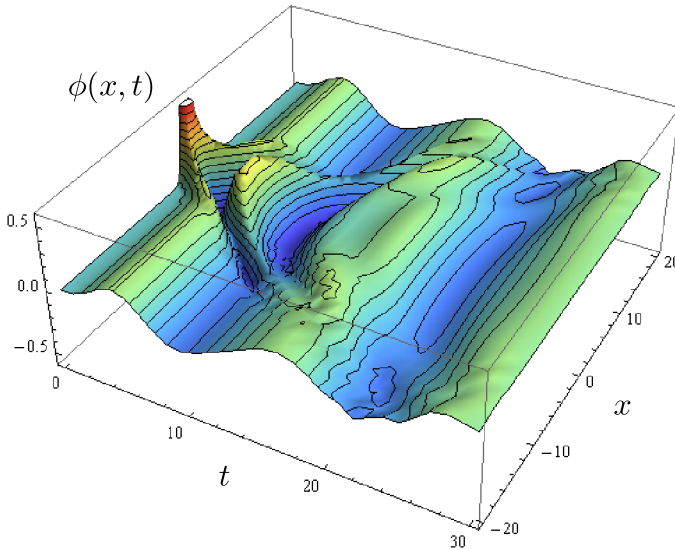
Figure 7. Numerical solution of the damped and temporally-forced SGE (18) in `Mathematica`® , with the following data (including the Gaussian initial state, zero initial velocity and symmetric boundary condition) $x \in [-20, 20]$, $t \in [0, 30]$, $\phi(x, 0) = \exp(-x^2)$, $\phi_t(x, 0) = 0$, $\phi(-20, t) = \phi(20, t)$, $\gamma = 0.2$, $F(x) = 0.1\sin(t/2)$. We can see the sine-forcing along all time axis. Damping of the SG-waves is also apparent.

2.4. SGE Modifications

2.4.1. SGE with Positive Sine Term

The simplest SGE modification is to replace the minus sine term with the plus sine

$$\phi_{tt} = \phi_{xx} + \sin\phi \qquad \text{or} \qquad \phi_{tt}(x,t) = \phi_{xx}(x,t) + \sin\phi(x,t). \qquad (17)$$

Again, a typical, spatially-symmetric, boundary-value problem for (17) is defined by

$$x \in [-L, L] \subset \mathbb{R}, \qquad t \in \mathbb{R}^+$$
$$\phi(x,0) = f(x), \quad \phi_t(x,0) = 0, \quad \phi(-L,t) = \phi(L,t)$$

where $f(x) \in \mathbb{R}$ is an axially-symmetric function (see Fig. 4).

2.4.2. Perturbed SGE and π–Kinks

As we have seen above (and it was proved by [3, 91]), the (1+1) SGE is integrable. In general though, the perturbations to this equation associated with the external forces and inhomogeneities spoil its integrability and the equation can not be solved exactly. Nevertheless, if the influence of these perturbations is small, the solution can be found perturbatively [40]. The perturbation theory for solitons was developed by [65] and subsequently applied by [79] to dynamics of vortices in Josephson contacts. Perturbed SGEs come in a variety of forms (see, e.g. [63–65, 79]).

One common form is a damped and driven SGE

$$\phi_{tt} + \gamma\phi_t - \phi_{xx} + \sin\phi = F \qquad (18)$$

where $\gamma\phi_t$ is the damping term and $F(x,t)$ is the spatiotemporal forcing. Special cases of the forcing term $F = F(x,t)$ in (18) are i) purely temporal $F = F(t)$ (e.g. periodic, see Fig. 6) ii) purely spatial $F = F(x)$ (e.g. central-symmetric, see Fig. 7) and iii) spatiotemporal $F = F(x,t)$ (e.g. temporally-periodic and spatially central-symmetric, see Fig. 8).

Considering (for simplicity) purely spatial forcing $F(x,t) = F(x)$, it has been shown in [36, 37] that if $F(x_0) = 0$ for some point $x_0 \in \mathbb{R}$, this can be an equilibrium position for the soliton. If there is only one zero, in case of a soliton this is a stable equilibrium position if $\left(\frac{\partial F(x)}{\partial x}\right)_{x_0} > 0$. In case of an antisoliton, this is a stable equilibrium position if $\left(\frac{\partial F(x)}{\partial x}\right)_{x_0} < 0$.
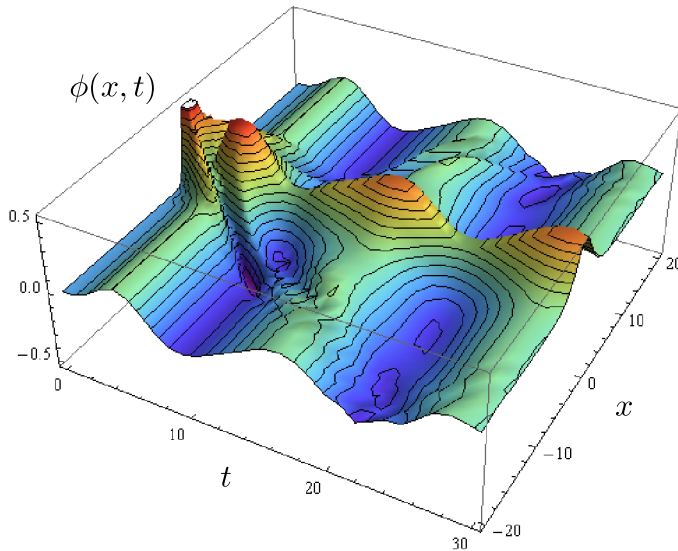
Figure 8. Numerical solution of the damped and both spatially and temporally forced SGE (18) in `Mathematica`® , with the following data (including the Gaussian initial state, zero initial velocity and symmetric boundary condition) $x \in [-20, 20]$, $t \in [0, 30]$, $\phi(x, 0) = \exp(-x^2)$, $\phi_t(x, 0) = 0$, $\phi(-20, t) = \phi(20, t)$, $\gamma = 0.2$, $F(x, t) = 0.1\sin(t/2) + 0.5\mathrm{sech}(x)$. We can see both temporal sine-forcing and spatial sech-forcing along all time axis. Damping of the SG-waves is still visible.

In particular if

$$F(x) = 2(\beta^2 - 1)\sinh(\beta x)/\cosh^2(\beta x), \qquad \beta \in \mathbb{R}$$

the exact stationary kink–solution of (18) is

$$\phi_k = 4 \arctan\left[\exp\left(\beta x\right)\right].$$

The stability analysis, which considers small amplitude oscillations around ϕ_k $\left[\phi(k, x) = \phi_k(x) + f(x)\mathrm{e}^{\lambda t}\right]$, leads to the following eigenvalue problem

$$\widehat{L}f = \Gamma f, \quad \text{where} \quad \widehat{L} = -\partial_x^2 + \left[1 - 2\cosh^{-2}(\beta x)\right] \quad \text{and} \quad \Gamma = -\lambda^2 - \gamma\lambda.$$

The eigenvalues of the discrete spectrum are given by the formula

$$\Gamma_n = \beta^2(\Lambda + 2\Lambda n - n^2) - 1$$

where $\Lambda(\Lambda + 1) = 2/\beta^2$. The integer part of Λ, yields the number of eigenvalues in the discrete spectrum, which correspond to the soliton modes (this includes the

translational mode Γ_0, and the internal or shape modes Γ_n with $n > 0$ (see [36, 37]).

In case of a function F defined in such a way that it possesses many zeroes, maxima and minima, perturbed SGE (18) describes an array of inhomogeneities. For example,

$$F(x) = \sum_{n=-q}^{q} 4\left(1 - \beta^2\right) \frac{\mathrm{e}^{\beta(x+x_n)} - \mathrm{e}^{3\beta(x+x_n)}}{\left(\mathrm{e}^{2\beta(x+x_n)} + 1\right)^2}$$

where $x_n = (n+2)\log\left(\sqrt{2}+1\right)/\beta$ $(n = -q, -q+1\cdots, q-1, q)$, and $q+2$ is the number of extrema points of $F(x)$. When the soliton is moving over intervals where $\frac{\mathrm{d}F(x)}{\mathrm{d}x} < 0$, its internal mode can be excited. The points x_i where $F(x_i) = 0$ and $\frac{\mathrm{d}F(x_i)}{\mathrm{d}x} < 0$, are 'barriers' which the soliton can overcome due to its kinetic energy (for more details, see [36, 37]).

Study of non-localized π-kinks in parametrically forced SGE (PSGE)

$$\phi_{tt} = \phi_{xx} - a(t/\epsilon)\sin\phi \qquad (19)$$

(over the fast time scale ϵ, where a is a mean-zero periodic function with a unit amplitude), has been performed by [114, 115], via 2π-kinks as approximate solutions. In particular, a finite-dimensional counterpart of the phenomenon of π-kinks in PSGE is the stabilization of the inverted *Kapitza pendulum* by periodic vibration of its suspension point. Geometrical averaging technique of [72] was applied as a series of canonical near-identical transformations via Arnold's normal form technique [6], as follows. Note that here the averaged forces in a rapidly forced system (e.g. inverted Kapitza pendulum) are the constraint forces of an associated auxiliary non-holonomic system and the curvature of these constraints enters the expression for the averaged system.

Starting with the Hamiltonian of PSGE (19), given by

$$H(\phi) = \int_{-\infty}^{+\infty}\left(\frac{p^2}{2} + \frac{\phi_x^2}{2} - a\cos\phi\right)\mathrm{d}x \qquad \text{where } p \equiv \phi_t \equiv \dot{\phi}$$

a series of canonical transformations was performed in [114] with the aim to kill all rapidly-oscillating terms, the following slightly-perturbed Hamiltonian was obtained

$$H_{\mathrm{per}} = \int_{-\infty}^{+\infty}\left(\frac{p_3^2}{2} + \frac{\phi_{3x}^2}{2} + \frac{1}{2}\epsilon^2\langle a_{-1}^2\rangle\sin^2\phi_3\right)\mathrm{d}x + O(\epsilon^3)$$

which, after rescaling $X = \epsilon x$, $T = \epsilon t$, $P = 2\epsilon^{-1}p_3$, $\Phi = 2\phi_3$, gave the following system of a slightly perturbed SGE with 2π-kinks as approximate solutions

$$\Phi_T = P + O(\epsilon^2), \qquad P_T = \Phi_{XX} - \langle a_{-1}^2\rangle\sin\Phi + O(\epsilon)$$

where a_{-1} is an anti-derivative with zero average. Finally, after rescaling back to variables (ϕ_3, p_3), approximate solutions $\phi_3 \approx \psi(x, t)$ in the form of π-kinks were obtained, with

$$\psi(x, t) = 2 \arctan \left[\exp \left(\epsilon \sqrt{\langle a_{-1}^2 \rangle} \frac{x - ct}{\sqrt{1 - c^2}} \right) \right]$$

where c is the wave-propagation velocity. For more technical details, see [114].

In addition, the following two versions of the perturbed SGE have been studied in [115]

1. Directly forced SGE

$$\phi_{tt} - \phi_{xx} + \sin \phi = M f(\omega t).$$

After shifting to the oscillating reference frame by the transformation

$$\phi = \theta + M \omega^{-2} F(\omega t) \tag{20}$$

where F has zero mean and $F''(\tau) = f(\tau)$, the parametrically forced ODE is obtained

$$\ddot{\theta} = -\sin \left(\theta + M \omega^{-2} F(\omega t) \right) \qquad \text{with}$$

$$H = \frac{p^2}{2} - A(\omega t) \cos(\theta) + B(\omega t) \sin(\theta) \tag{21}$$

where p is the momentum canonically conjugate to θ, and

$$A(\omega t) = \cos(M \omega^{-2} F(\omega t)), \qquad B(\omega t) = \sin(M \omega^{-2} F(\omega t)).$$

From (21), the corresponding evolution PDE (in canonical form) is obtained for a new phase θ on top of a rapidly oscillating background field

$$\theta_t = p, \qquad p_t = \theta_{xx} - \sin \left(\theta + M \omega^{-2} F(\omega t) \right).$$

After retracing the identical transformation (20), the so-obtained (approximate) solutions become π-kinks (see [115] for technical details).

2. Damped and driven SGE

$$\phi_{tt} - \phi_{xx} + \sin \phi = M f(\omega t) - \alpha \phi_t + \eta \tag{22}$$

which is frequently used to describe long Josephson junctions [79]. In (22), ϕ represents the phase-difference between the quantum-mechanical wave

functions of the two superconductors defining the Josephson junction, t is the normalized time measured relative to the inverse plasma frequency, x is space normalized to the Josephson penetration depth, while $Mf(\omega t)$ represents tunneling of superconducting Cooper pairs (normalized to the critical current density).

Starting with a homogeneous transformation to the oscillating reference frame, analogous to (20) and designed to remove the free oscillatory term $\phi = \theta + G(t)$, and substituting this transformation to (22), while choosing the function G so that it solves the following ODE

$$\ddot{G} + \alpha \dot{G} = Mf(\omega t)$$

the following evolution PDE is obtained (in canonical form) [115]

$$\theta_t = p, \qquad p_t = \theta_{xx} - \alpha p + \eta - \sin(\theta + G(\omega t)). \qquad (23)$$

For the particular case of $f(\tau) = \sin \tau$, the function G is found to be

$$G(\tau) = -\frac{\alpha}{\omega} \frac{M}{\alpha^2 + \omega^2} \cos \tau - \frac{M}{\alpha^2 + \omega^2} \sin \tau.$$

After a series of transformations (related to a directly-forced pendulum), in zeroth order in α, η, the evolution PDE (23) reduces (after neglecting terms $\sim \omega^{-3}$) to SGE, which has π-kink solutions. Therefore, slightly perturbed π-kinks are approximate solutions of the original equation (22) (on top of the rapidly oscillating background field, see [115] for technical details).

2.4.3. SGE in (2+1) Dimensions

The (2+1)D SGE with additional spatial coordinate (y) is defined on $\mathbb{R}^{2,1}$ as

$$\varphi_{tt} = \Delta \varphi - \sin \varphi = \varphi_{xx} + \varphi_{yy} - \sin \varphi. \qquad (24)$$

In the case of a long Josephson junction, the soliton solutions of (24) describe Josephson vortices or *fluxons*. These excitations are associated with the distortion of a Josephson vortex line and their shapes can have an arbitrary profile, which is retained when propagating. In (24), φ denotes the superconducting phase difference across the Josephson junction. The coordinates x and y are normalized by the Josephson penetration length λ_J, and the time t is normalized by the inverse Josephson plasma frequency ω_p^{-1} (see [41] and references therein).

A special class of solutions of (24) can be constructed by generalization of the solution of (1) which does not depend on one of the coordinates, or, obtained by

Lorentz transforming the solutions of a stationary 2D SGE. However, there are numerical solutions of (24) which cannot be derived from the (1) or (3), e.g. radial breathers (pulsons) [41].

A more general class of solutions of the (2+1)D SG equation has the following form

$$\varphi(x, y, t) = 4 \arctan \exp \left[y - f(x \pm t) \right] \tag{25}$$

which exactly satisfies (24) with an arbitrary real-valued twice-differentiable function $f = f(x \pm t)$.

Because of the arbitrariness of f, solution (25) describes a variety of excitations of various shapes. Choosing f localized in a finite area, e.g. $f = A / \cosh(x - t)$, solution (25) describes an excitation, localized along x that keeps its shape when propagating, i.e., a solitary wave (in the sense of [91]). For each solitary wave of this type, there exists an anti-partner with an f of opposite sign in (25). For solitary waves to be solitons, there is an additional important criterion restoring their shapes after they collide.

Consider a trial function

$$\varphi(x, y, t) = 4 \arctan \exp \left[y - f(x + t) \pm f(x - t) \right]$$

that, when $t \to -\infty$, describes the propagation of two solitary shape waves toward each other (minus sign) or a solitary wave and its anti-partner (plus sign). One can see that (25) can only *approximately* satisfy (24) when $|f'(x + t) f'(x - t)| \ll 1$ for all values of x and t. This suggests that, in general, the condition for restoring the shapes may not be satisfied. In general case, (24) can not be satisfied, that prompts that the collision of two solitary waves leads to distortion of the original excitations [41].

The excitations, described by f in (25) are similar to elastic shear waves in solid mechanics [34]. Since the equation (24) is Lorentz-covariant, we can obtain other solutions performing Lorentz transformations on (25), which leads to a class of solutions of the form [41]

$$\varphi(x, y, t) = 4 \arctan \exp \left[\frac{y - v\, t}{\sqrt{1 - v^2}} - f \left(x \pm \frac{t - v\, y}{\sqrt{1 - v^2}} \right) \right].$$

2.4.4. Two Coupled SGEs

The following two-parameter system of two coupled SGEs was introduced by [66]

$$\phi_{tt} - \phi_{xx} = -\beta^2 \sin(\phi - \psi) \tag{26}$$
$$\psi_{tt} - \alpha^2 \psi_{xx} = \sin(\phi - \psi), \qquad \text{with constants } \alpha, \beta > 0.$$
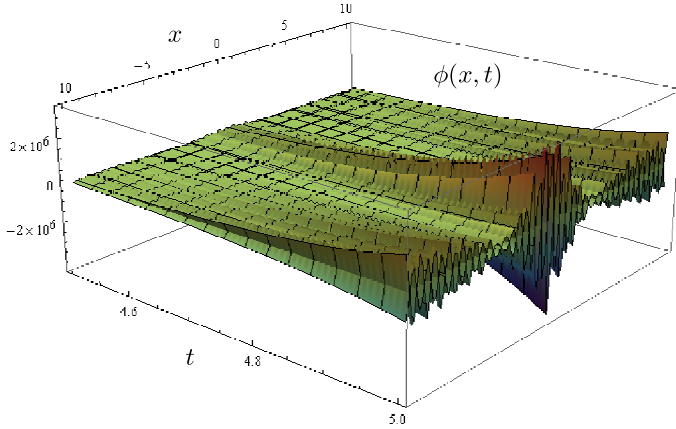
Figure 9. Numerical solution of the SGE-system (26) in `Mathematica`®, with the following data $x \in [-10, 10]$, $t \in [0, 5]$, $\alpha = 0.5$, $\beta = 0.3$, $\phi(x, 0) = 0.3 \exp(-x^2)$, $\psi(x, 0) = 0.7 \exp(-x^2)$, $\phi_t(x, 0) = 0$, $\phi(-10, t) = \phi(10, t)$, $\psi_t(x, 0) = 0$, $\psi(-10, t) = \psi(10, t)$.

For numerical solution, see Fig. 9.

The SGE-system (26) has been exactly solved by [92], where (using a series of substitutions) it was first reduced to the nonlinear second-order ODE

$$\varphi''(\xi) = \left[\frac{1 + \alpha^2 \beta^2 - c^2 \left(1 + \beta^2\right)}{\left(c^2 - 1\right)\left(c^2 - \alpha^2\right) \mu^2} + \frac{2\varphi'^2}{\varphi(\xi)^2 + 1} \right] \varphi(\xi) \qquad (27)$$

equivalent to the following autonomous system in the $(X, Y) -$ plane

$$\frac{\mathrm{d}X}{\mathrm{d}\xi} = Y, \qquad \frac{\mathrm{d}Y}{\mathrm{d}\xi} = \left[\frac{1 + \alpha^2 \beta^2 - c^2 \left(1 + \beta^2\right)}{\left(c^2 - 1\right)\left(c^2 - \alpha^2\right) \mu^2} + \frac{2Y^2}{X^2 + 1} \right] X. \qquad (28)$$

System (28) has an equilibrium point at the origin $(X, Y) = (0, 0)$, in which the Jacobian matrix is

$$J_{(0,0)} = \begin{pmatrix} 0 & 1 \\ \lambda & 0 \end{pmatrix} \qquad \text{with} \qquad \lambda = \frac{\alpha^2 \beta^2 - c^2 \left(1 + \beta^2\right) + 1}{\left(c^2 - 1\right)\left(c^2 - \alpha^2\right) \mu^2}.$$

The phase portraits from this system show that there exist periodic solutions of the coupled SGEs (26).

Using the exponential ansatz

$$\varphi(\xi) = \frac{p \exp(\xi) + q \exp(-\xi)}{r \exp(\xi) + s \exp(-\xi)}, \qquad \text{with constants } p, q, r, s \in \mathbb{R}$$

four pairs of analytic solutions of the system (27), and therefore of the system (26), were found in [92]. We present here only the first two (simpler) solution pairs

$$\phi_1(x,t) = \frac{\beta^2}{4\left(c^2 - 1\right)\mu^2}\sin(2\xi) + c_1\xi + c2$$

$$\psi_1(x,t) = \frac{\beta^2}{4\left(c^2 - 1\right)\mu^2}\sin(2\xi) + c_1\xi + c2 - 2\arctan(\tan(\xi))$$

$$\xi = \mu(x - ct), \qquad c = \sqrt{\frac{1 - \alpha^2\beta^2}{1 - \beta^2}}$$

and

$$\phi_2(x,t) = \frac{\beta^2}{4\left(c^2 - 1\right)\mu^2}\sin(2\xi) + c_1\xi + c2$$

$$\psi_2(x,t) = \frac{\beta^2}{4\left(c^2 - 1\right)\mu^2}\sin(2\xi) + c_1\xi + c2 - 2\arctan(\cot(\xi))$$

$$\xi = \mu(x - ct), \qquad c = \sqrt{\frac{1 - \alpha^2\beta^2}{1 - \beta^2}}\,.$$

For more technical details, see [92].

2.5. Sine–Gordon Chain and Discrete Breathers

2.5.1. Frenkel–Kontorova Model

The original Frenkel–Kontorova model [9, 10, 33] of stationary and moving crystal dislocations, was formulated historically decades before the continuous SGE. It consists of a chain of harmonically coupled atoms in a spatially periodic potential, governed by the set of differential-difference equations

$$\ddot{\phi}_n + \frac{1}{\Delta x^2}\left[\phi_{n+1} - 2\phi_n + \phi_{n-1}\right] + \sin\phi_n = 0 \tag{29}$$

where ϕ_n denotes the position of the nth atom in the chain. Alternatively, system (29) represents a chain of torsionally-coupled pendula (see Fig. 2), where ϕ_n is the angle which the nth pendulum makes with the vertical.

2.5.2. Sine–Gordon Chain

To derive dynamical equations of the sine–Gordon chain (SGC), consisting of anharmonic oscillators with the coupling constant μ, we start with the three-point,

central, finite-difference approximation of the spatial derivative term ϕ_{xx} in the SGE

$$\phi_{xx} \approx \frac{1}{\Delta x^2} \left[\phi_{n+1} - 2\phi_n + \phi_{n-1} \right] + O(x^2)$$
$$= -\frac{1}{\Delta x^2} \left[(\phi_n - \phi_{n-1}) - (\phi_{n+1} - \phi_n) \right] + O(x^2).$$

Applying this finite-difference approximation to the SGE (1), and also performing the corresponding replacements $\phi \to \phi_n$, $\phi_{tt} \to \ddot{\phi}_n$ and $\mu = 1/\Delta x^2$, we obtain the set of difference ODEs defining the SGC

$$\ddot{\phi}_n + \mu \left[(\phi_n - \phi_{n-1}) - (\phi_{n+1} - \phi_n) \right] + \sin \phi_n = 0. \tag{30}$$

The system (30) describes a chain of interacting particles subjected to a periodic on-site potential $V(x) = \sin(x)$. In the continuum limit, (30) becomes the standard SGE (1) and supports stable propagation of a kink-soliton of the form (14).
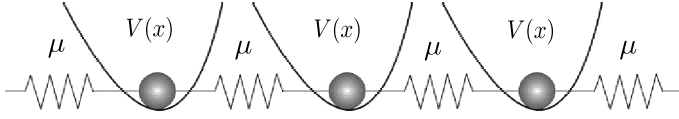
Figure 10. Simple sine–Gordon chain (SGC) with the coupling constant μ and the periodic on-site potential $V(x) = \sin(x)$.

The linear-wave spectrum of (30) around a kink has either one or two localized modes (which depends on the value of μ) [90]. The frequencies of these modes lie inside the spectrum gap. The linear spectrum, with the linear frequency ω and the wave number k, is given by

$$\omega^2 = 1 + 4\mu \sin^2 \frac{k}{2} \tag{31}$$

while the gap edge frequency is $\omega = 1$.

The simplest example of (30), containing only two oscillators, is defined by [90]

$$\ddot{\phi}_{1,2} + \mu(\phi_{1,2} - \phi_{2,1}) + \sin \phi_{1,2} = 0. \tag{32}$$

It was demonstrated in [38], using the method of averaging in fast oscillations, that a perturbed SGC, damped and driven by a large-amplitude ac-force, might support localized kink solitons. Specifically, they considered the perturbed SGC

$$\ddot{\phi}_n - \mu \left[\phi_{n+1} - 2\phi_n + \phi_{n-1} \right] + \sin \phi_n = \chi + \alpha \sin \omega t - \gamma \dot{\phi}_n \tag{33}$$

where χ is a dc-force, α and ω are the normalized (large) amplitude and frequency of a periodic force, respectively, while γ is the normalized dissipative coefficient. Without the forcing on the right-hand side, (33) reduces to (30).

2.5.3. Continuum Limits

Perturbed SGEs have their corresponding perturbed SGCs. The following 0-π SGC was proposed in [20]

$$\ddot{\phi}_n = \frac{\phi_{n-1} - 2\phi_n + \phi_{n+1}}{a^2} - \sin(\phi_n + \theta_n) + \gamma \tag{34}$$

as an equation of a phase ϕ_n-motion (of a 0-π array of Josephson junctions). Here, a is the lattice spacing parameter, $\gamma > 0$ is the applied bias current density, and $\theta_n = (0$ if $n \leq 0$ and $-\pi$ if $n > 0)$ is the phase jump of π in ϕ_n. The SGC equation (34) is derived from the following discrete Lagrangian

$$L_{\mathrm{D}} = \int \sum_{n \in \mathbb{Z}} \left[\frac{1}{2} \left(\frac{\mathrm{d}\phi_n}{\mathrm{d}t} \right)^2 - \frac{1}{2} \left(\frac{\phi_{n+1} - \phi_n}{a} \right)^2 - 1 + \cos(\phi_n + \theta_n) + \gamma \phi_n \right] \mathrm{d}t. \tag{35}$$

In the continuum limit $a \ll 1$ Lagrangian (35) becomes

$$L_{\mathrm{C}} = \iint_{-\infty}^{\infty} \left[\frac{1}{2} (\phi_t)^2 - \frac{1}{2} \left(\widetilde{L}_a \phi_x \right)^2 - 1 + \cos(\phi + \theta) + \gamma \phi \right] \mathrm{d}x \, \mathrm{d}t$$

from which, the continuum limit of (34) gives the following perturbed SGE

$$\phi_{tt} = L_a \phi_{xx} - \sin(\phi + \theta) + \gamma$$

where $\theta = (0$ if $x \leq 0$ and $-\pi$ if $x > 0)$, while the differential operators $L_a \phi_{xx}$ and $\widetilde{L}_a \phi_x$ are given by the following Taylor expansions

$$L_a \phi_{xx} = \frac{\phi_{n-1} - 2\phi_n + \phi_{n+1}}{a^2} = 2 \sum_{k=0}^{\infty} \frac{a^{2k}}{(2k+2)!} \partial_{xx}^k \phi_{xx}(na)$$

$$\widetilde{L}_a \phi_x = \frac{\phi_{n+1} - \phi_n}{a} = \sum_{k=0}^{\infty} \frac{a^k}{(k+1)!} \partial_x^k \phi(na).$$

For more technical details, including several other continuum limits, see [20].

2.5.4. Discrete Breathers

Generally speaking, it is a well-known fact (see, e.g. [30] and references therein) that different types of *excitations*, most notably *phonons* (propagating linear waves) and *discrete breathers* (DBs for short which are time-periodic spatially localized excitations, also labeled intrinsic localized modes or discrete solitons) can occur as solutions of spatially-discrete nonlinear lattices. According to S. Flach *et*

al [28, 30, 32] DBs are caused by a specific interplay between the nonlinearity and discreteness of the lattice. The lattice nonlinearity provides with an amplitude-dependent tunability of oscillation or rotation frequencies of DBs, while its spatial discreteness leads to finite upper bounds of the frequency spectrum of small amplitude waves. DBs are not sensitive to specific types of nonlinearities in the lattice nor are they confined to any lattice dimensions. They are (usually) dynamically and structurally stable and emerge in a variety of physical systems (ranging from lattice vibrations and magnetic excitations in crystals to light propagation in photonic structures and cold atom dynamics in periodic optical traps, see [31]). Although DBs present complex dynamical objects, experimental measurements can (in many cases) be well understood by using their *time-averaged* properties (see [78]). In addition, nonlinear discrete lattices admit different types of DBs depending on the spectrum of linear waves propagating in the lattice [7,28,29,32], including acoustic breathers, rotobreathers and optical breathers (see Fig. 11).
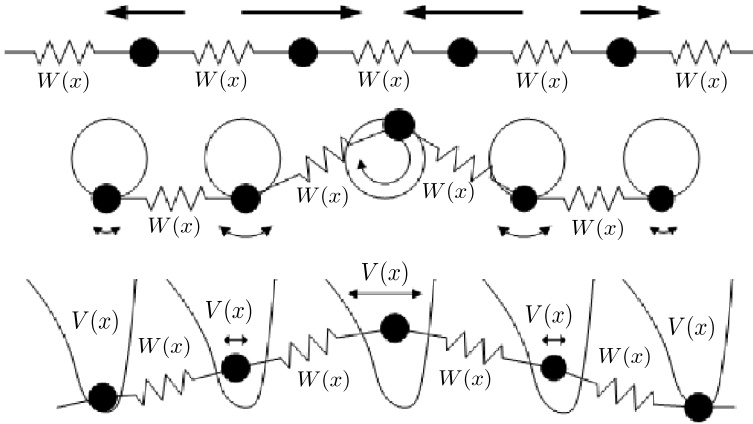
Figure 11. Different types of discrete breathers (DBs): acoustic breather (top), rotobreather (middle), and optical breather (bottom). Modified and adapted from [7, 28, 29, 32]).

A particular system studied in [28,31] has been characterized by the lattice Hamiltonian

$$
\begin{aligned}
H &= \sum_{n} \left[\frac{1}{2}\dot{x}_n^2 + W(x_n - x_{n-1}) + V(x_n) \right] \\
&= \sum_{n} \left[\frac{1}{2}p_n^2 + W(x_n - x_{n-1}) + V(x_n) \right]
\end{aligned}
\tag{36}
$$

where $x_n = x_n(t)$ are time-dependent coordinates with canonically-conjugate momenta $p_n = \dot{x}_n(t)$, $W(x_n) = W(x)$ is the nearest neighbor interaction, and $V(x_n) = V(x)$ is an optional on-site (substrate) potential. From (36) the following equations of motion are derived

$$\ddot{x}_n = -W'(x_n - x_{n-1}) + W'(x_{n+1} - x_n) - V'(x_n) \qquad \text{or}$$

$$\dot{x}_n = \dot{x}_n, \qquad \dot{p}_n = -W'(x_n - x_{n-1}) + W'(x_{n+1} - x_n) - V'(x_n)$$

where (for simplicity) the following zero initial conditions are assumed

$$V(0) = W(0) = V'(0) = W'(0) = 0, \qquad V''(0) \geq 0, \qquad W''(0) > 0.$$

Hamiltonian (36) supports the excitation of small amplitude linear waves

$$x_n(t) \sim \exp\left[\mathrm{i}(\omega_q t - qn)\right]$$

with the wave number q and the corresponding frequency spectrum ω_q^2 which, due to the underlying lattice, depends periodically on q

$$\omega_q^2 = V''(0) + 4W''(0)\sin^2\left(\frac{q}{2}\right)$$

and its absolute value has always a finite upper bound. The maximum (Debye) frequency of small amplitude waves is

$$\omega_q = \sqrt{V''(0) + 4W''(0)}\,.$$

DBs exist for different types of potentials $W(x)$ and $V(x)$. DB solutions are [28] i) time-periodic $\hat{x}_n(t + T_b) = \hat{x}_n(t)$, and ii) spatially localized $\hat{x}_{|n|\to\infty} \to 0$. In addition, if the Hamiltonian H is invariant under a finite translation/rotation of any $x_n \to x_n + \lambda$, then *discrete rotobreathers* may exist (see [103]), which are excitations characterized by one or several sites in the breather center evolving in a rotational state $\hat{x}_0(t + T_b) = \hat{x}_0(t) + \lambda$, while outside this center the lattice is governed again by time periodic spatially localized oscillations.

3. Sine–Gordon Solitons, Kinks and Breathers in Living Cellular Structures

In this section, we give the applications of the sine–Gordon equation (and the variety of its traveling–wave solutions), as spatiotemporal models of nonlinear excitations in living cellular structures.

3.1. SGE Solitons in DNA

In this subsection, we review the first three papers describing SGE–solitary excitations in DNA. The idea that it is possible that soliton excitations may suggest a discovery of a new mechanism in the duplication of DNA and the transcription of messenger ribonucleic acid (mRNA) goes back to [25], who demonstrated the existence of transiently open states in DNA and synthetic polynucleotide double–helices, by hydrogen exchange measurements.

The first two papers in this domain were published by [110] and [113] – incidentally, under the same title, in the same journal (PRA), using two slightly-different modifications of the same coupled SGE–system (26).

Note that, in the same period, Yakushevich *et al* performed their SGE–solitary studies of DNA (see [108, 109] and references therein), focusing on the effects of weak inhomogeneities in simple DNA fragments (consisting of uniform base sequences of a given type followed by uniform base sequence of the other type), which were described in terms of a parametrically–perturbed SGE.

Note that, according to the standard Watson–Crick double–helix $B-$form DNA model, the two polynucleotide strands forming a double helix are held together by hydrogen H-bonds. Yomosa was assuming that the H-bonding and the stacking energies (consisting of the electrostatic, the exchange, the charge-transfer, as well as the induction and dispersion interactions), were roughly proportional to the overlaps of molecular orbitals.

Firstly, Yomosa considered in [110] (see also [111]) the Watson–Crick $B-$form model, in which the zero-level of the energies E_B and E_S are taken for the $B-$form of DNA and polynucleotide duplexes, while the mean energy of distorted double and triple H-bonds in $A - T$ (adenine–thymine) and $G - C$ (guanine–cytosine) base pairs is approximately represented (by the formula for molecular association in liquids by [89]) for the energy of a distorted single H-bond. In this model the conformation and stability of DNA and the polynucleotide double helices are determined by

1. The energy E_B of the hydrogen H-bonds between inter-strand complementary base pairs, given by

$$E_B = \sum_n B[1 - \cos(\theta_n - \theta'_n - \pi)]$$

where B is a parameter associated with the H-bond energy, while $\theta_n = \angle(B_n, P_n)$ and $\theta'_n = \angle(B'_n, P'_n)$ denote angles between horizontal projections of the complementary base pairs and their corresponding axes, and

2. The stacking energy E_S between intra-strand adjacent bases, given by

$$E_S = \sum_n S[1 - \cos(\theta_n - \theta_{n-1} - \alpha_0)] + S[1 - \cos(\theta'_n - \theta'_{n-1} - \alpha_0)]$$

where S is a parameter associated with the stacking energy of DNA chains and $\alpha_0 = 36°$.

Next, by adding the rotational kinetic energy

$$T_{\text{rot}} = \frac{1}{2} \sum_n I[\dot{\theta}_n^2 + \dot{\theta}'^2_n]$$

(where I is the mean value of the moments of inertia I_n of the bases for the rotations around the axes P) to the potential energies E_B and E_S, the following SG–chain Hamiltonian for DNA and synthetic polynucleotide double–helices was formulated

$$H = T_{\text{rot}} + E_B + E_S = \frac{1}{2} \sum_n I[\dot{\theta}_n^2 + \dot{\theta}'^2_n] + \sum_n B[1 - \cos(\theta_n - \theta'_n - \pi)]$$

$$+ \sum_n \left\{ S[1 - \cos(\theta_n - \theta_{n-1} - \alpha_0)] + S[1 - \cos(\theta'_n - \theta'_{n-1} - \alpha_0)] \right\}. \tag{37}$$

From the Hamiltonian (37), via canonical Hamiltonian formalism, the following two sets of coupled SGC–equations of motion were derived in [110]

$$I\ddot{\theta}_n + B\sin(\theta_n - \theta'_n - \pi) + S[\sin(\theta_n - \theta_{n-1} - \alpha_0) - \sin(\theta_{n+1} - \theta_n - \alpha_0)] = 0$$
$$I\ddot{\theta}'_n + B\sin(\theta_n - \theta'_n - \pi) + S[\sin(\theta'_n - \theta'_{n-1} - \alpha_0) - \sin(\theta'_{n+1} - \theta'_n - \alpha_0)] = 0.$$

Further, by linearizing this coupled ODE-system (assuming the smallness of the angles $\theta_n - \theta_{n-1} - \alpha_0$ and $\theta'_n - \theta'_{n-1} - \alpha_0$) and subsequently performing the continuum limit

$$\theta_n(t) \to \theta(x,t), \qquad \theta'_n(t) \to \theta'(x,t). \tag{38}$$

Yomosa derived the following system of two coupled SGEs, of the (slightly-modified) form of (26)

$$I\theta_{tt} - S\theta_{xx} = -B\sin(\theta - \theta' - \pi)$$
$$I\theta'_{tt} - S\theta'_{xx} = B\sin(\theta - \theta' - \pi). \tag{39}$$

Unfortunately, in his time, Yomosa was not able solve the coupled system (39), so he took the difference of the two SGEs and obtained the following single SGE representing a dynamic (plane) base-rotator model

$$\frac{1}{v_0^2}\phi_{tt} = \phi_{xx} - \frac{1}{l^2}\sin\phi, \qquad \text{where} \quad v_0 = \sqrt{S/I}, \qquad l = \sqrt{S/2B}. \tag{40}$$

Finally, by imposing the following boundary condition

$$\cos\phi = 1 \quad \text{for} \quad \phi = 2\pi n, \quad n = 0, \pm 1, ...$$
$$\text{at} \ \xi = \pm\infty \quad \text{at} \ x = \pm\infty \quad \text{for all} \ t$$

the following traveling solitary-wave solutions of (40) were obtained in the form (11) of a *kink–antikink* pair

$$\phi(x,t) = 4 \arctan \exp\left[\pm\frac{(\xi - \xi_0)}{\sqrt{1 - v/v_0^2}l}\right].$$

Secondly, Zhang clarified in [113] the pioneering (and therefore somewhat-messy) approach of Yomosa and proposed the following modified SGC–Hamiltonian for the $B-$form DNA double–helix (rewritten here in above Yomosa's notation for consistency)

$$H = \frac{1}{2}\sum_n I[\dot\theta_n^2 + \dot\theta_n'^2] + \sum_n V(\theta_n, \theta_n')$$
$$+ \frac{1}{2}\sum_n \left[S(\theta_n - \theta_{n-1})^2 + S(\theta_n' - \theta_{n-1}')^2\right] \tag{41}$$

where $V(\theta_n, \theta_n')$ is the inter-strand interaction energy in nth base pair, given by

$$V(\theta_n, \theta_n') = B[1 - \cos(\theta_n - \theta_n')] + \lambda(1 - \cos\theta_n) + \lambda(1 - \cos\theta_n')$$
$$+ \beta\left\{3(1 - \cos\theta_n \cos\theta_n') - [1 - \cos(\theta_n - \theta_n')]\right\}$$

where the zero-level of the energy is taken for the $B-$form DNA, the same way as Yomosa did. From the Hamiltonian (41), the following SGC–equations of motion were derived in [113]0

$$I\ddot\theta_n + B\sin(\theta_n - \theta_n') + \beta[3\sin\theta_n\cos\theta_n' - \sin(\theta_n - \theta_n')] + \lambda\sin\theta_n$$
$$= S(\theta_{n+1} - 2\theta_n + \theta_{n-1}) \tag{42}$$
$$I\ddot\theta_n' - B\sin(\theta_n - \theta_n') + \beta[3\cos\theta_n\sin\theta_n' + \sin(\theta_n - \theta_n')] + \lambda\sin\theta_n'$$
$$= S(\theta_{n+1}' - 2\theta_n' + \theta_{n-1}').$$

By performing the approximation (38), Zhang introduced the continuum variables θ and θ'. Subsequently, by introducing new variables $\phi = \theta + \theta'$, $\psi = \theta - \theta'$, he obtained the following system of two perturbed and coupled SGEs

$$\phi_{xx} - (1/c_0^2)\phi_{tt} = (1/l^2)\sin\phi + (2/\alpha^2)\sin(\phi/2)\cos(\psi/2)$$
$$\psi_{xx} - (1/c_0^2)\psi_{tt} = (1/l^2)\sin\psi + (2/\alpha^2)\sin(\psi/2)\cos(\phi/2)$$
$$\text{where} \quad c_0 = \sqrt{S/I}, \qquad l = \sqrt{S/(3\beta)}, \qquad \alpha = \sqrt{S/\lambda}$$

which cannot be solved analytically. So, by setting $\lambda = 0$ in (42), Zhang arrived at the following system of two independent SGEs (with $Q = (2B + \beta)/(3\beta)$

$$\phi_{xx} - (1/c_0^2)\phi_{tt} = (1/l^2)\sin\phi$$
$$\psi_{xx} - (1/c_0^2)\psi_{tt} = (Q/l^2)\sin\psi \tag{43}$$

with the simple solution of a single soliton with velocity c,

$$\phi_0^{\pm}(x,t) = 4\arctan\exp\left(\pm z\right), \qquad \psi_0^{\pm}(x,t) = 4\arctan\exp\left(\pm\sqrt{Q}\,z\right) \tag{44}$$

where

$$z = (\gamma/l)(\xi - \xi_0), \qquad \xi = x - ct, \qquad \gamma = 1/\sqrt{1 - c^2/c_0^2}.$$

Finally, by returning to original continuum variables θ and θ', from (44), Zhang obtained a set of π-kink/antikink and 2π-kink/antikink solutions (see [113] for more technical details).

The third (and most-cited) paper in this domain (of SGE–solitary excitations in DNA) was Salerno [93] (see also [94, 95]), who proposed a discrete SGC model for DNA-promoter dynamics. He introduced the following SGC–Hamiltonian (slightly refined from Yomosa's and Zhang's Hamiltonians)

$$H = \frac{1}{2}\sum_{n=1}^{N} I[\dot{\psi}_n^2 + \dot{\theta}_n^2] + \sum_{n=1}^{N} K\left[(\psi_{n+1} - \psi_n)^2 + (\theta_{n+1} - \theta_n)^2\right]$$
$$+ \sum_{n=1}^{N} \eta_n[1 - \cos(\psi_n - \theta_n)] \tag{45}$$

where N is the number of base-pairs in the SGC and K is the backbone spring constant along both DNA–helices. η_n is a nonlinear parameter used to model the strength of H-bonds between complementary bases, chosen according to the following rule $\eta_n = \lambda_n\beta$ with $\lambda_n = 2$ if it refers to $A - T$ or $T - A$ pairs, $\lambda_n = 3$ otherwise, with β a free parameter. From the Hamiltonian (45), the following SGC–equations of motion were derived

$$I\ddot{\psi}_n = K(\psi_{n+1} - 2\psi_n + \psi_{n-1}) - \frac{\beta}{2}\lambda_n\sin(\psi_n - \theta_n)$$
$$I\ddot{\theta}_n = K(\theta_{n+1} - 2\theta_n + \theta_{n-1}) - \frac{\beta}{2}\lambda_n\sin(\theta_n - \psi_n). \tag{46}$$

Further, from (46), the following SGC–equation of motion is obtained for the angle difference $\phi_n = \psi_n - \theta_n$, between complementary bases

$$\ddot{\phi}_n = \phi_{n+1} - 2\phi_n + \phi_{n-1} - \frac{\beta}{K}\lambda_n\sin\phi_n. \tag{47}$$

We remark that the ODE (47) has the standard form of (30) and from it, in the continuum limit, the standard SGE (1) is obtained, with exact soliton solutions (as described in the Subsection 2.3.1. before). Salerno used the ODE–model (47) to study nonlinear wave dynamics of the $T7A1-$DNA promoter (see [93] for further technical details).

3.2. SGE Solitons in Protein Folding

For over a decade, it has been known that nonlinear excitations can influence conformational dynamics of biopolymers. E.g. the effective bending rigidity of a biopolymer chain could lead to a buckling instability [77]. Subsequently, several models have been proposed to explain such protein transition (see, e.g. [101] and references therein).

In this subsection, we review two protein–folding dynamics papers. Firstly, it was suggested in [12] that protein folding may be mediated via interaction of the protein (molecular) chain with SGE–solitons which propagate along the chain. Local potential energy of the chain is modeled by an asymmetric double-well potential

$$V(\varphi) = \varepsilon(\varphi + \delta)^2(\varphi^2 - \frac{2}{3}\varphi\delta + \frac{1}{3}\varphi^2 - 2)$$

where the scalar variable φ represents local conformation of the protein, ε is a small positive parameter, while δ is the asymmetry parameter (ranging from -1 to $+1$). The two minima of the potential, corresponding to the local α- and β-conformations of the chain, are positioned at $\varphi = \pm 1$ and the energy-difference between them is $\Delta E = \frac{16}{3}\varepsilon\delta$.

Solitonic excitations are realized in [12] by an additional, dissipative SGE–field $\phi(x)$, where x is the position along the protein. The following interaction potential (with the positive parameter Λ) is used to mediate interaction between the two fields

$$u(\phi, \varphi) = \frac{\Lambda}{\Lambda + 1}(1 - \cos\phi)\varphi^2.$$

The following dissipative equations of motion are derived [12]

$$\phi_{tt} = \phi_{xx} - \frac{1 + \Lambda\varphi^2}{1 + \Lambda}\sin\phi - \gamma_\phi\phi_t$$

$$m\varphi_{tt} = -4\varepsilon(\varphi + \delta)(\varphi^2 - 1) - \frac{2\Lambda}{1 + \Lambda}\varphi(1 - \cos\phi) - \gamma_\varphi\varphi_t$$

(48)

where $\gamma_\phi\phi_t$ and $\gamma_\varphi\varphi_t$ are dissipative terms. In the small interaction limit (ignoring $\gamma_\phi\phi_t$), it is chosen

$$\phi(x, t) = f(x - vt) + \Delta\theta(x, t), \qquad \varphi(x, t) = 1 + \Delta\varphi(x, t)$$

where $f(z) = 4 \arctan(e^{-z})$ is the usual SGE–kink, moving with velocity v. For $\varphi(x,t)$, the following approximate sech–soliton solution is obtained

$$\Delta \varphi \simeq - \frac{4\Lambda/m}{v^2 + (\omega/2)^2} \frac{1}{\cosh^2(x - vt)}.$$

So, near the center of the ϕ kink, φ is pushed away from its local minima $\varphi = 1$ towards the other local minima. A localized static solution of (48) is found to be

$$\phi = 4\tan^{-1} \frac{1}{q + \sqrt{1 + q^2}}, \qquad \varphi^2 = 1 - \frac{\Lambda}{\varepsilon(1 + \Lambda)} \frac{1}{1 + q^2}$$

where $q \equiv \sqrt{1 - a} \, \sinh(x - x_0)$, $a = \Lambda^2/[2\varepsilon(1+\Lambda)^2]$ (for more technical details, see [12]).

More recently, a Lagrangian field–theory based modeling approach to protein folding has been proposed in [62]. They proposed the protein Lagrangian including three terms

   i) nonlinear unfolding ϕ^4-protein at the initial state

$$\mathcal{L}_{\text{unf}} = \frac{1}{2}(\partial_\mu \phi)^\dagger (\partial^\mu \phi) + \frac{m_\phi^4}{\lambda_\phi} \left[1 - \cos(\frac{\sqrt{\lambda_\phi}}{m_\phi}|\phi|) \right]$$

   ii) nonlinear sources injected into the backbone, modeled by ψ^4 self-interaction

$$\mathcal{L}_{\text{src}} = \frac{1}{2}(\partial_\mu \psi)^\dagger (\partial^\mu \psi) + \frac{\lambda_\psi}{4!}(\psi^\dagger \psi)^2$$

   iii) the interaction term (with the coupling constant Λ)

$$\mathcal{L}_{\text{int}} = -\Lambda \, (\phi^\dagger \phi)(\psi^\dagger \psi).$$

The total potential (from all three terms) reads

$$V_{\text{tot}}(\phi, \psi) = \frac{m_\phi^4}{\lambda_\phi} \left[1 - \cos(\frac{\sqrt{\lambda_\phi}}{m_\phi}|\phi|) \right] + \frac{\lambda_\psi}{4!}(\psi^\dagger \psi)^2 - \Lambda \, (\phi^\dagger \phi)(\psi^\dagger \psi).$$

Assuming that λ_ϕ is small enough to be approximately at the same order with λ_ψ, the first term can be expanded in term of $\sqrt{\lambda_\psi}$, giving (up to the second order accuracy)

$$V_{\text{tot}}(\phi, \psi) \approx \frac{m_\phi^2}{2} \phi^\dagger \phi - \frac{\lambda_\phi}{4!}(\phi^\dagger \phi)^2 + \frac{\lambda_\psi}{4!}(\psi^\dagger \psi)^2 - \Lambda \, (\phi^\dagger \phi)(\psi^\dagger \psi)$$

from which the total Lagrangian $\mathcal{L}_{\text{tot}} = \mathcal{L}_{\text{unf}} + \mathcal{L}_{\text{src}} + \mathcal{L}_{\text{int}}$ can be (up to the second order accuracy) approximated by

$$
\begin{aligned}
\mathcal{L}_{\text{tot}}(\phi, \psi) = {} & \frac{1}{2} \left[(\partial_\mu \phi)^\dagger (\partial^\mu \phi) + (\partial_\mu \psi)^\dagger (\partial^\mu \psi) \right] \\
& + \frac{m_\phi^2}{2} \phi^\dagger \phi - \frac{\lambda_\phi}{4!} (\phi^\dagger \phi)^2 + \frac{\lambda_\psi}{4!} (\psi^\dagger \psi)^2 - \Lambda (\phi^\dagger \phi)(\psi^\dagger \psi).
\end{aligned}
\tag{49}
$$

From the Euler–Lagrangian PDEs for the total Lagrangian (49)

$$
\frac{\partial \mathcal{L}_{\text{tot}}}{\partial |\phi|} - \partial_\mu \frac{\partial \mathcal{L}_{\text{tot}}}{\partial (|\partial_\mu \phi|)} = 0, \qquad \frac{\partial \mathcal{L}_{\text{tot}}}{\partial |\psi|} - \partial_\mu \frac{\partial \mathcal{L}_{\text{tot}}}{\partial (|\partial_\mu \psi|)} = 0
$$

the following coupled and perturbed SGE and (nonlinear) KGE with cubic forcing are derived

$$
\phi_{tt} = \phi_{xx} - \frac{m_\phi^3}{\sqrt{\lambda_\phi}} \sin(\frac{\sqrt{\lambda_\phi}}{m_\phi} |\phi|) + 2\Lambda |\phi||\psi|^2
\tag{50}
$$

$$
\psi_{tt} = \psi_{xx} - \frac{\lambda_\psi}{6} |\psi|^3 + 2\Lambda |\psi||\phi|^2
\tag{51}
$$

where $\lambda_\phi-$ and $\lambda_\psi-$terms determine nonlinearities of backbone and source, respectively.

Numerical solution of the two coupled (1+1) PDEs, (50)–(51), with the following boundary conditions

$$
\begin{aligned}
&\phi(0, t) = \phi(L, t) = 0 \ \text{ and } \ \psi(0, t) = \psi(L, t) = 0 \ \text{ for } 0 \le t \le b \\
&\phi(x, 0) = p(x) \ \text{ and } \ \psi(x, 0) = f(x) \qquad\qquad\quad \text{ for } 0 \le x \le L \\
&\phi_t(x, 0) = q(x) \ \text{ and } \ \psi_t(x, 0) = g(x) \qquad\qquad\quad \text{ for } 0 < x < L
\end{aligned}
\tag{52}
$$

(where $p(x)$, $q(x)$, $f(x)$ and $g(x)$ are auxiliary functions), would describe the contour of conformational changes for protein folding. It was performed in [62] using the following forward finite differences

$$
\begin{aligned}
\phi_{i,j+1} = {} & 2\phi_{i,j} - \phi_{i,j-1} + \Delta t^2 \big(\frac{\phi_{i+1,j} - 2\phi_{i,j} + \phi_{i-1,j}}{\Delta x^2} + 2\Lambda \psi_{i,j}^2 \phi_{i,j} \\
& - \frac{m_\phi^3}{\hbar^3 \sqrt{\lambda_\phi}} \sin(\frac{\sqrt{\lambda_\phi}}{m_\phi} \phi_{i,j}) \big) \\
\psi_{i,j+1} = {} & 2\psi_{i,j} - \psi_{i,j-1} \\
& + \Delta t^2 \big(\frac{\psi_{i+1,j} - 2\psi_{i,j} + \psi_{i-1,j}}{\Delta x^2} + 2\Lambda w_{i,j}^2 \psi_{i,j} - \frac{\lambda_\psi}{6} \psi_{i,j}^3 \big)
\end{aligned}
$$

where the values at the first time-step t_1 are given by the boundary conditions (52), while the values at the second time-step t_2 are determined by the 2nd-order Taylor expansion

$$\phi_{i,2} = p_i - \Delta t q_i + \frac{1}{2}\Delta t^2 (\frac{p_{i+1} - 2p_i + p_{i-1}}{\Delta x^2} + 2\Lambda f_i^2 p_i$$

$$- \frac{m_\phi^3}{\hbar^3 \sqrt{\lambda_\phi}} \sin(\frac{\sqrt{\lambda_\phi}}{m_\phi} p_i)) \qquad \text{for} \; i = 2, 3, \cdots, N-1$$

$$\psi_{i,2} = f_i - \Delta t g_i + \frac{1}{2}\Delta t^2 (\frac{f_{i+1} - 2f_i + f_{i-1}}{\Delta x^2} + 2\Lambda p_i^2 f_i - \frac{\lambda_\psi}{6} f_i^3).$$

For more technical details, see [62].

3.3. SGE Solitons in Microtubules

In this subsection, we review two most-significant papers describing SGE–solitary excitations in microtubules (MTs) and then point-out to some related quantum studies of neural MTs.

MTs are major cytoskeletal proteins assembled from the tubulin protein that plays a crucial role in all eukaryotic cells. MT functions include cellular orientation, structure and guidance of membrane and cytoplasmic movement, which are crucial effects to cell division, morphogenesis, and embryo development. MT structure is a hollow cylinder that typically involves 13 protofilaments (of protein dimers called tubulins). Each protofilament is formed from tubulin molecules arranged in a 'head-to-tail joint' fashion. The inner and the outer diameters of the cylinder are 15nm and 25nm, while its length may span dimensions from the order of micrometer to the order of millimeter. Each dimer is an electric dipole whose length and longitudinal component of the electric dipole moment are 8nm and 337Debye, respectively. The constituent parts of the dimers are α and β tubulins, corresponding to positively and negatively charged sides, respectively (see [22], as well as references in [96–98, 112]).

3.3.1. Soliton Dynamics in MTs

To the best of our knowledge, the first paper describing soliton dynamics in MTs was [96] (cf also [97, 98, 112], for a recent review, see [54]), in which Satarić *et al* developed a ferroelectric model of neural MTs where the motion of MT subunits is reduced to a single longitudinal DOF per dimer at a position n, denoted by ϕ_n. The overall effect of the surrounding dimers on a dipole at a chosen site n can be

qualitatively described by the following double-well quartic potential

$$V(\phi_n) = -\frac{1}{2}A\phi_n^2 + \frac{1}{4}B\phi_n^4 \tag{53}$$

where A and B are real parameters (A is a linear function of temperature). As an electrical dipole, a dimer in the intrinsic electric field of the MT acquires the additional potential energy given by

$$V_{\text{el}} = -qE\phi_n$$

where $q = 18 \times 2e$ (e = electron charge) denotes the effective mobile charge of a single dimer and E is the magnitude of the intrinsic electric field. In addition, two more MT–related energies can also be defined

i) the potential energy of restoring strain–forces between adjacent dimers in the protofilament (with a unique spring/stiffness constant k)

$$V_{\text{str}} = \frac{1}{2}k(\phi_{n+1} - \phi_n)^2 \qquad \text{and}$$

ii) the (velocity $\dot{\phi}_n$−dependent) kinetic energy associated with the longitudinal displacements of constituent dimers with unique mass m

$$T(\dot{\phi}_n) = \frac{1}{2}\sum_{n=1}^{N} m\dot{\phi}_n^2$$

where N is the total number of constituent dimers in the *microtubular chain* (MTC).

The full MTC–Hamiltonian is now given by

$$\begin{aligned}
H &= T(\dot{\phi}_n) + V_{\text{str}} + V(\phi_n) + V_{\text{el}} \\
&= \sum_{n=1}^{N}\left[\frac{1}{2}m\dot{\phi}_n^2 + \frac{1}{2}k(\phi_{n+1} - \phi_n)^2 - \frac{1}{2}A\phi_n^2 + \frac{1}{4}B\phi_n^4 - qE\phi_n\right].
\end{aligned} \tag{54}$$

Also, in order to derive a realistic equation of motion for the MTC, it is indispensable to include the viscous force $F_{\text{v}}(\dot{\phi}_n) = -\gamma\dot{\phi}_n$, with the damping coefficient γ. We remark here that the friction γ should be viewed as an environmental effect, which does not lead to energy dissipation which is a well-known result, relevant to energy transfer in biological systems [69].

Using the Hamiltonian (54) together with the damping force $F_{\mathrm{v}}(\dot{\phi}_n)$, and subsequently performing the continuum limit (with equilibrium spacing r_0 between adjacent dimers)

$$\phi_n(t) \rightarrow \phi(x, t)$$

$$\phi_{n+1}(t) \rightarrow \phi(x, t) + r_0\phi_x(x, t) + \frac{1}{2}r_0^2\phi_{xx}(x, t) + \dots$$

– Satarić *et al* finally derived their nonlinear (forced and damped) wave equation

$$m\phi_{tt} + \gamma\phi_t - kr_0^2\phi_{xx} = A\phi - B\phi^3 + qE. \tag{55}$$

The importance of the electric force term qE lies in the fact that the PDE (55) admits soliton solutions with no energy loss, which acquires the form of a traveling wave, and can be expressed by defining a normalized displacement field [69]

$$\psi(\xi) = \frac{\phi(\xi)}{\sqrt{A/B}} \quad \text{with } \xi = \alpha(x - vt), \qquad \alpha = \sqrt{\frac{|A|}{m(v_0^2 - v^2)}}$$

where $v_0 = \sqrt{k/m}r_0$ is the sound velocity and v is the soliton–propagation velocity. In terms of the $\psi(\xi)$ variable, the wave equation (55) reduces to a damped anharmonic oscillator ODE

$$\psi'' + \rho\psi'^3 + \psi + \sigma = 0 \qquad \text{where} \tag{56}$$
$$\rho = \gamma v[m|A|(v_0^2 - v^2)]^{-\frac{1}{2}}, \qquad \sigma = q\sqrt{B}|A|^{-3/2}E$$

which has a unique bounded solution [96]

$$\psi(\xi) = a + \frac{b - a}{1 + \exp\left(\frac{b-a}{\sqrt{2}}\xi\right)} \qquad \text{such that} \tag{57}$$

$$(\psi - a)(\psi - b)(\psi - d) = \psi^3 - \psi - \left(\frac{q\sqrt{B}}{|A|^{3/2}}E\right). \tag{58}$$

So the kink propagates along the protofilament axis with fixed velocity

$$v = v_0/\sqrt{1 + 2\gamma^2/(9d^2m|A|)}$$

which depends on the strength of the electric field E via (58). The total *conserved energy* of the kink (57) is given by

$$E = \frac{2\sqrt{2}}{3}\frac{A^2}{B} + \frac{\sqrt{2}}{3}k\frac{A}{B} + \frac{1}{2}m^*v^2 \qquad \text{where}$$
$$m^* = \frac{4}{3\sqrt{2}}\frac{mA\alpha}{r_0B} \qquad \text{is kink's } \textit{effective} \text{ mass.} \tag{59}$$

The first term of (59) expresses the binding energy of the kink and the second the resonant transfer energy (note that in realistic biological models, the sum of these two terms dominate over the third term, being of order of 1eV).

For the further development of the theory, with kink-antikink waves traveling in opposite directions along the MTC, see [75, 96–98, 112].

Now, from our general SGE perspective, Satarić model (55) can be approximated by the perturbed SGE (18), rewritten here for our readers' convenience

$$\phi_{tt} + \gamma\phi_t - \phi_{xx} + \sin\phi = F$$

and if we apply the following assumptions

i) normalized units $m = k = r_0 = 1$

ii) electrical force $qE = F \equiv F(x, t)$

iii) using the (first two terms of the) Taylor–series expansion of the sine term

$$\sin\phi = \phi - \frac{1}{6}\phi^3 + O(\phi^4) \approx A\phi - B\phi^3. \tag{60}$$

Using assumptions i)–ii) and approximation (60), all results of the Section 2.4.2. (illustrated with the simulation Figures 4–8) are ready to be employed for the further SGE analysis of solitary excitations in microtubules.

The second paper describing soliton dynamics in MTs was [13]. Under similar assumptions as [96], they proposed the same expresions for the kinetic energy $T(\dot{\phi}_n)$ and potential energy V_{str} of restoring strain–forces between adjacent dimers. However, in contrast to the quartic potential (53), Chou *et al* followed the recipes from solid state physics [21] and expressed the interaction for the nth tubulin molecule of a protofilament by the following periodic (effective) potential

$$V(\phi_n) = V_0 \left[1 - \cos(\frac{2\pi\phi_n}{a_0}) \right]$$

where V_0 is the half-height of the potential energy barrier, ϕ_n is the displacement of the nth tubulin molecule within a particular protofilament and $a_0 = 8$nm is the distance between the centers of two neighboring tubulin molecules along a protofilament. In this way, they defined the following MTC–Hamiltonian

$$\begin{aligned} H &= T(\dot{\phi}_n) + V_{\mathrm{str}} + V(\phi_n) \\ &= \sum_{n=1}^{N} \left[\frac{1}{2}m\dot{\phi}_n^2 + \frac{1}{2}k(\phi_{n+1} - \phi_n)^2 + V_0(1 - \cos\frac{2\pi\phi_n}{a_0}) \right]. \end{aligned} \tag{61}$$

Using canonical Hamilton's equations, from (61) they derived the MTC–equations of motion for the nth tubulin molecule within a protofilament (for $n = 1, 2, ...N$)

$$m\ddot{\phi}_n = k(\phi_{n+1} - 2\phi_n + \phi_{n-1}) - \frac{2\pi V_0}{a_0} \sin \frac{2\pi\phi_n}{a_0} . \tag{62}$$

In the continuum limit $\phi_n(t) \to \phi(x, t)$, the MTC–equations of motion (62) reduce to the SGE

$$m\phi_{tt} = ka_0^2\phi_{xx} - (\frac{2\pi}{a_0})^2 V_0 \sin \phi \qquad \text{or}$$

$$\phi_{tt} = \frac{1}{c^2}\phi_{xx} - \frac{1}{l^2}\sin\phi \quad \text{with} \quad c^2 = \frac{ka_0^2}{m}, \qquad \frac{1}{l^2} = \frac{4\pi^2 V_0}{ka_0^4} \tag{63}$$

which is the same SGE as (43) that was used by [113] for DNA–solitons, with kink–antikink solutions (44). Using (63), Chou *et al* showed that there was a very high and narrow peak at the center of the kink width, implying that a tubulin molecule would have its maximum momentum when it reaches the top of the periodic potential (for more technical details, see [13]).

In particular, in the case of *neural* MTs, possibility for sub-neuronal processing of information by cytoskeletal *tubulin tails* has been proposed by [35], by showing that local electromagnetic field supports information that could be converted into specific protein tubulin-tail conformational states. Long-range collective coherent behavior of the tubulin tails could be modeled in the form of sine-Gordon kinks, antikinks or breathers that propagate along the microtubule outer surface, and the tubulin-tail soliton collisions could serve as elementary computational gates that control cytoskeletal processes. The authors of [35] have used the results of [1], combined with the *elastic ribbon* SGE–*model* of [21]. Applying Bäcklund transformations (4) they found two- and three-soliton solutions, as well as their elastic collisions. They developed *Maple*®-based animations of a whole 'zoo' of colliding solitons, including kink/antikink pairs and three types of breathers i) a standing breather, ii) a traveling large amplitude breather and iii) a traveling small amplitude breather.

We remark that standing breather soliton could be obtained *in vivo* in experiments in which the electric-field vector acts perpendicular to the microtubule $z-$ axis. If a local vortex of the electromagnetic field is created somewhere in the neuron, then the exerted action of the electric field vector along the z-axis will be zero and no traveling soliton would be born. This standing breather, swinging at certain tubulin tail could catalyze attachment/detachment of microtubule associated proteins and promote or inhibit the kinesin walk.

3.3.2. The Liouville Stringy Arrow of Time in Neural MTs

Now, recall that the term cubic in ψ in the equation of motion (56) was responsible for the appearance of a kink-like classical solution. Let us formulate a Liouville $(1 + 1)-$string theory of the neural MT–complex, following [75], and consider a general polynomial in T equation of motion for a static tachyon

$$T''(\xi) + \rho T'(\xi) = P(T) \tag{64}$$

(where ξ is some space-like coordinate and $P(T)$ is a polynomial of degree n), in which the 'friction' term T' expresses a Liouville derivative. In this interpretation of the Liouville field as a local scale on the world-sheet it is natural to assume that the single-derivative term expresses the non-critical string β-function, and hence is itself a polynomial R of degree m $T'(\xi) = R(T)$. Such equations lead to kink-like solutions [86]

$$T(\xi) = \frac{1}{2a_4}\{\text{sgn}(a_2 a_4)a_2 \text{tanh}[\frac{1}{2}a_2(x - vt)] - a_2\} \tag{65}$$

where

$$v = \frac{A_3 - 3a_2 a_4}{a_4} \quad \text{is the velocity}$$

which is a universal behavior for biological systems [69], showing the existence of a scheme which admits kink–like solutions for energy transfer without dissipation in cells. The structure of the equation (64), which leads to kink-like solutions (65), is generic for Liouville strings in non-trivial background space-times.

According to the conventional *Liouville theorem* (which is usually derived from the continuity equation $\rho_t+ \text{div}(\rho\,\dot{\mathbf{x}}) = 0$) written here in terms of Poisson brackets $\{\cdot,.\}$

$$\rho_t = -\{\rho, H\} \tag{66}$$

the phase-space density of the field theory associated with the matter DOF of the MT–complex evolves with time as a consequence of phase-space volume-preserving symmetries. More generally, statistical description of the temporal evolution of the MT–complex using classical density matrices $\rho(\phi^i, t)$ [24]

$$\rho_t = -\{\rho, H\} + \beta^i G_{ij}\partial_{p_j}\rho \tag{67}$$

where p_i are momenta canonically-conjugate to the fields ϕ^i, and G_{ij} is the metric in the space of fields $\{\phi^i\}$. The non-Hamiltonian term in (67) leads to a violation of

the Liouville theorem (66) in the classical phase space $\{\phi^i, p_j\}$, and constitutes the basis for a dissipative quantum-mechanical description of the system [24], upon density-matrix quantization. In string theory, summation over world sheet surfaces will imply quantum fluctuations of the string target-space background fields ϕ^i.

Using Dirac's quantization rule $\{.,.\} \longrightarrow -\mathrm{i}\,[.,.]$, the quantum version of (67) reads (in terms of the quantum commutator $[.,.]$, see [24])

$$\hat{\rho}_t = \mathrm{i}[\hat{\rho}, \hat{H}] + \mathrm{i}\beta^i G_{ij}[\hat{\phi}^i, \hat{\rho}] \tag{68}$$

where the hat denotes quantum operators, and appropriate *quantum ordering* (in the sense of [73]) is understood. In (68), $\hat{H}$ is the Hamiltonian evolution operator, while

$$\hat{\rho} = \sum_a P(a)\, |\Psi_a\rangle \langle \Psi_a| \qquad \text{with} \qquad \mathrm{Tr}(\hat{\rho}) = 1$$

is von Neumann's *density matrix* operator, in which each quantum state $|\Psi_a\rangle$ occurs with probability $P(a)$ and von Neumann's entropy is defined as

$$S = -\mathrm{Tr}(\hat{\rho}[\ln \hat{\rho}]).$$

The very structure of the quantum Liouville equation (68) implies the following properties of the MT–complex [23, 24, 84]

　i) conservation of probability P

$$P_t = \mathrm{Tr}_t(\hat{\rho}) = 0$$

　ii) conservation of average energy $\langle E\rangle$, $\langle E\rangle_t \equiv \mathrm{Tr}_t(\hat{\rho}E) = (p_i\beta^i)_t = 0$ and

　iii) monotonic increase in entropy S

$$S_t \equiv -\mathrm{Tr}_t(\hat{\rho}\ln\hat{\rho}) = S(\beta^i G_{ij}\beta^j) \geq 0$$

　　which naturally implies a microscopic arrow of time within the MT–complex [84].

However, the quantum energy fluctuations

$$\delta E \;\equiv\; [\langle\langle\mathcal{H}^2\rangle\rangle - (\langle\langle\mathcal{H}\rangle\rangle)^2]^{\frac{1}{2}}$$

are time-dependent and actually decrease with time [75]

$$\partial_t(\delta E)^2 = -\mathrm{i}\langle\langle[\beta^i, \mathcal{H}]\beta^j G_{ji}\rangle\rangle = \langle\langle\beta^j G_{ji}\frac{\mathrm{d}\beta^i}{\mathrm{d}t}\rangle\rangle$$
$$= -\langle\langle Q^2\beta^i G_{ij}\beta^j\rangle\rangle = -\langle\langle Q^2\partial_t C\rangle\rangle \;\leq 0.$$

3.4. SGE Solitons in the Conduction of Neural Impulse

Recently, two biophysicists from the Niels Bohr Institute in Copenhagen, Heimburg and Jackson (see [43,44]), challenged the half-a-century old electrical theory of neural impulse conduction, proposed by A. Hodgkin and A. Huxley in the form of their celebrated HH equations (1963 Nobel Prize in Physiology or Medicine). The HH model, which relies on ionic currents through ion channel proteins and the membrane capacitor, is the presently accepted textbook model for the nerve impulse conduction.

For our readers' reference, here is a brief on the HH model, which (in its basic form) consists of four coupled nonlinear first-order ODEs, including the cable equation for the neural membrane potential V, together with m, h and n equations for the gating variables of Na and K channels and leakage (cf [47,48] and for recent reviews, see [42,61])

$$C_m \dot{V} = -g_{\mathrm{Na}} m^3 h (V - V_{\mathrm{Na}}) - g_{\mathrm{K}} n^4 (V - V_{\mathrm{K}}) - g_{\mathrm{L}} (V - V_{\mathrm{L}}) + I_j^{\mathrm{ext}}$$
$$\dot{m} = -\left(a_m + b_m\right) m + a_m, \qquad \dot{h} = -\left(a_h + b_h\right) h + a_h \qquad (69)$$
$$\dot{n} = -\left(a_n + b_n\right) n + a_n$$

where

$$a_m = 0.1\,(V + 40)/[1 - \mathrm{e}^{-(V+40)/10}], \qquad b_m = 4\,\mathrm{e}^{-(V+65)/18}$$
$$a_h = 0.01\,(V + 55)/[1 - \mathrm{e}^{-(V+55)/10}], \qquad b_h = 0.125\,\mathrm{e}^{-(V+65)/80}$$
$$a_n = 0.07\,\mathrm{e}^{-(V+65)/20}, \qquad b_n = 1/[1 + \mathrm{e}^{-(V+35)/10}].$$

Here the reversal potentials of Na, K channels and leakage are $V_{\mathrm{Na}} = 50$ mV, $V_{\mathrm{K}} = -77$ mV and $V_{\mathrm{L}} = -54.5$ mV. The maximum values of corresponding conductivities are $g_{\mathrm{Na}} = 120$ mS/cm^2, $g_{\mathrm{K}} = 36$ mS/cm^2, $g_{\mathrm{L}} = 0.3$ mS/cm^2 and the capacity of the membrane is $C_m = 1$ μF/cm^2. The external, input current is given by

$$I_j^{\mathrm{ext}} = g_{\mathrm{syn}}(V_a - V_c) \sum_n \alpha(t - t_{\mathrm{in}}) \qquad (70)$$

which is induced by the pre-synaptic spike-train input applied to the neuron i, given by $U_i(t) = V_a \sum_n \delta(t - t_{\mathrm{in}})$. In (70), t_{in} is the nth firing time of the spike-train inputs, g_{syn} and V_c denote the conductance and the reversal potential, respectively, of the synapse, τ_{s} is the time constant relevant to the synapse conduction, and $\alpha(t) = (t/\tau_{\mathrm{s}})\,\mathrm{e}^{-t/\tau_{\mathrm{s}}}\Theta(t)$ (where $\Theta(t)$ is the Heaviside function).

In addition, Hodgkin and Huxley assumed that the total current is the sum of the trans-membrane current and the current along the axon and that a propagating solution exists that fulfills a wave equation, so the simple cable ODE figuring in the

basic HH model (69) was further expanded into the following PDE for the propagating nerve impulse depending on the axon radius a

$$\frac{a}{2R_i}V_{xx} = C_m V_t + g_{\text{K}}(V - E_{\text{K}}) + g_{\text{Na}}(V - E_{\text{Na}})$$

where R_i is the resistance of the cytosol within the nerve (see [44] for technical review).

The HH model was originally proposed to account for the property of squid giant axons [47,48] and it has been generalized with modifications of ion conductances. More generally, the HH–type models have been widely adopted for a study on activities of *transducer neurons* such as motor and thalamus relay neurons, which transform the amplitude-modulated input to spike-train outputs. For attempts to relate the HH model (as well as its simplified form, Fitzhugh–Nagumo model (FHN) [27, 81]) with propagation of solitons in neural cell membranes see [15] and references therein.

Among several forms of the FHN–model, the simplest one (similar to the Van der Pol oscillator) is suggested by FitzHugh himself in [27]

$$\epsilon \frac{dx}{d\tau} = \epsilon \dot{x} = x - x^3 - y$$
$$\frac{dy}{d\tau} = \dot{y} = \gamma x - y + b$$

where x is voltage (the fast variable), y is the slow recovery variable and γ, b, ϵ ($0 \leq \epsilon \ll 1$) are parameters.

However, the HH model fails to explain a number of features of the propagating nerve pulse, including the reversible release and reabsorption of heat. Electrical currents through resistors generate heat, independent of the direction of the ion flux; the heat production in the HH–model should always be positive, while the heat dissipation should be related to the power of a circuit through the resistor, i.e., $\dot{Q} = P = V.I > 0$ (for each of the conducting objects in all phases of the action potential, see [43,44]). Similar case is with the accompanying mechanical, fluorescence, and turbidity changes [43,44]

> "The most striking feature of the isothermal and isentropic compression modulus is its significant undershoot and striking recovery. These features lead generically to the conclusions i) that there is a minimum velocity of a soliton and ii) that the soliton profiles are remarkably stable as a function of the soliton velocity. There is a maximum amplitude and a minimum velocity of the solitons that is close to the propagation velocity in myelinated nerves..."

Earlier work of Hill [5] (the previous English Nobel laureate for physiology and the president of the Royal Society London during the II World War), on heat production in nerves (which was based on his previous work on heat production in contracted muscles [46]) is actually reviewed in [48], where it is noted that the heat release and absorption response during the action potential is important 'but is not understood'.

Based on thermodynamic relation between heat capacity and membrane area compressibility, Heimburg and Jackson considered in [43, 44] a (1+1) hydrodynamic PDE for the dispersive sound propagation in a cylindrical membrane of a density-pulse, governing the changes $\Delta\rho^A$ (along the x-axis) of the lateral membrane density ρ^A, defined by $\Delta\rho^A(x,t) = \rho^A(x,t) - \rho_0^A$, where $\rho_0^A = 4.035.10^{-3}\,g/m^2$ is the equilibrium lateral area density in the fluid phase of the membrane slightly above the melting point. The related sound velocity c can be expanded into a power series (close to the lipid melting transition) as

$$c^2 = c_0^2 + p(\Delta\rho^A) + q(\Delta\rho^A)^2 + \ldots \tag{71}$$

where $c_0 = 176.6$ m/s is the velocity of small amplitude sound, while p and q are parameters ($p = -16.6\,c_0^2/\rho_0^A$ and $q = 79.5\,c_0^2/(\rho_0^A)^2$).

In our standard $\phi-$notation, with $\phi(x,t) \equiv \Delta\rho^A(x,t)$, the *dispersive wave equation* of [43, 44] can be written as

$$\phi_{tt} = c^2\phi_{xx} - f(\phi). \tag{72}$$

Here, we need to make two remarks regarding the dispersive wave equation (72)

1. If the compressibility is approximately constant and if $\Delta\rho^A \ll \rho_0^A$, then the dispersive force $f(\phi)$ is zero and (72) reduces to the standard wave equation (depending only on the small amplitude sound c_0^2)

$$\phi_{tt} = c_0^2\phi_{xx}\,.$$

2. If higher sound frequencies (resulting in higher propagation velocities as the isentropic compressibility is a decreasing function of frequency) become dominant, the dispersive forcing function $f(\phi)$ in (72) needs to be defined, or *ad-hoc chosen* [43, 44] to mimic the linear frequency–dependence of the sound velocity with a positive parameter h as $f(\phi) = h\phi_{xxxx}$. In this case, the expansion (71) needs to be explicitly included into PDE (72), resulting in the equation governing dispersive sound propagation, which reads (in original notation of [43, 44])

$$\frac{\partial^2}{\partial t^2}\Delta\rho^A = \frac{\partial}{\partial x}\left[\left(c_0^2 + p(\Delta\rho^A) + q(\Delta\rho^A)^2\right)\frac{\partial}{\partial x}\Delta\rho^A\right] - h\frac{\partial^4}{\partial x^4}\Delta\rho^A. \tag{73}$$

Furthermore, by introducing the sound propagation velocity v, after the coordinate transformation $z = x - v \cdot t$, the dispersive PDE (73) can be recast into a time-independent form, describing the *shape* of a propagating density excitation

$$v^2 \frac{\partial^2}{\partial z^2} \Delta \rho^A = \frac{\partial}{\partial z} \left[\left(c_0^2 + p(\Delta \rho^A) + q(\Delta \rho^A)^2 \right) \frac{\partial}{\partial z} \Delta \rho^A \right] - h \frac{\partial^4}{\partial z^4} \Delta \rho^A.$$

This one-dimensional PDE has a localized (stationary) solution [70]

$$\Delta \rho^A(z) = \frac{p}{q} \cdot \frac{1 - \left(\frac{v^2 - v_{min}^2}{c_0^2 - v_{min}^2} \right)}{1 + \left(1 + 2\sqrt{\frac{v^2 - v_{min}^2}{c_0^2 - v_{min}^2}} \cosh \left(\frac{c_0}{h} z \sqrt{1 - \frac{v^2}{c_0^2}} \right) \right)}$$

which is a *sech-type soliton,* a typical solution for KdV and NLS equations.

Now, without arguing either pro- or contra- Heimburg–Jackson theory of *neural sound propagation,* as an alternative to Hodgkin–Huxley *electrical theory,* we will simply accept the natural solitary explanation of the nerve impulse conduction, regardless of the physical medium that is carrying it (sound, or heat, or electrical, or smectic liquid crystal [15], or possibly quantum-mechanical [75]). However, we are free to chose a different form for the dispersive force term $f(\phi)$ in the perturbed wave equation (72). For example, instead of the Heimburg–Jackson's ad-hoc choice of the forth-derivative term, following [96] and subsequent studies of neural MTs, we can choose a double-well quartic dispersive potential (53), which will, combined with the approximation (60), result in the standard SGE (1), generating analytical solutions of the traveling soliton, kink-antikink and breather form (as described in the Subsection 2.3.1. above).

3.5. Muscular Contraction Solitons on Poisson Manifolds NLS, KdV and SGE

For geometrical analysis of nonlinear PDEs, instead of using common symplectic structures arising in ordinary Hamiltonian mechanics, the more appropriate approach is a *Poisson manifold* $(\mathfrak{g}^*, \{\cdot, \cdot\})$, in which $\mathfrak{g}^*$ is a chosen Lie algebra with a $(\pm)$ *Lie–Poisson bracket* $\{F, G\}_{\pm}(\mu))$ and carries an abstract *Poisson evolution equation* $\dot{F} = \{F, H\}$. This approach is well–defined in both the finite– and the infinite–dimensional case (see [51, 52, 59, 76]).

Let E_1 and E_2 be Banach spaces. A continuous bilinear functional $\langle , \rangle : E_1 \times E_2 \to \mathbb{R}$ is nondegenerate if $\langle x, y \rangle = 0$ implies $x = 0$ and $y = 0$ for all $x \in E_1$ and $y \in E_2$. We say E_1 and E_2 are in *duality* if there is a nondegenerate bilinear

functional $\langle\,,\,\rangle : E_1 \times E_2 \to \mathbb{R}$. This functional is also referred to as an $L^2-pairing$ of E_1 with E_2.

Recall that a *Lie algebra* consists of a vector (e.g. Banach) space $\mathfrak{g}$ carrying a bilinear skew–symmetric operation $[\,,\,] : \mathbf{g} \times \mathbf{g} \to \mathbf{g}$, called the *commutator* or Lie bracket. This represents a pairing $[\xi, \eta] = \xi\eta - \eta\xi$ of elements $\xi, \eta \in \mathfrak{g}$ and satisfies *Jacobi identity*

$$[[\xi,\eta],\mu] + [[\eta,\mu],\xi] + [[\mu,\xi],\eta] = 0.$$

Let $\mathfrak{g}$ be a (finite– or infinite–dimensional) Lie algebra and $\mathfrak{g}^*$ its dual Lie algebra, that is, the vector space L^2 paired with $\mathfrak{g}$ *via* the inner product $\langle\,,\,\rangle : \mathfrak{g}^* \times \mathfrak{g} \to \mathbb{R}$. If $\mathfrak{g}$ is finite–dimensional, this pairing reduces to the usual action (interior product) of forms on vectors. The standard way of describing any finite–dimensional Lie algebra $\mathfrak{g}$ is to provide its n^3 *structural constants* γ_{ij}^k, defined by $[\xi_i, \xi_j] = \gamma_{ij}^k \xi_k$, in some basis ξ_i, $(i = 1, \dots, n)$.

The $(\pm)$ Lie–Poisson bracket (75) is a bilinear and skew–symmetric operation. It also satisfies the Jacobi identity

$$\{\{F,G\},H\}_\pm(\mu) + \{\{G,H\},F\}_\pm(\mu) + \{\{H,F\},G\}_\pm(\mu) = 0$$

(thus confirming that $\mathfrak{g}^*$ is a Lie algebra), as well as the Leibniz rule

$$\{FG,H\}_\pm(\mu) = F\{G,H\}_\pm(\mu) + G\{F,H\}_\pm(\mu). \tag{74}$$

Also, for any two smooth functions $(F,G) : \mathfrak{g}^* \to \mathbb{R}$, we define the *Fréchet derivative D* on the space $L(\mathfrak{g}^*, \mathbb{R})$ of all linear diffeomorphisms from $\mathfrak{g}^*$ to $\mathbb{R}$ as a map $DF : \mathfrak{g}^* \to L(\mathfrak{g}^*, \mathbb{R})$, $\mu \mapsto DF(\mu)$. Further, we define the *functional derivative $\delta F/\delta\mu \in \mathfrak{g}$* by

$$DF(\mu) \cdot \delta\mu = \langle\delta\mu, \frac{\delta F}{\delta\mu}\rangle$$

with arbitrary 'variations' $\delta\mu \in \mathfrak{g}^*$.

Now, for any two smooth functions $F, G : \mathfrak{g}^* \to \mathbb{R}$, we define the $(\pm)$ *Lie–Poisson bracket* by

$$\{F,G\}_\pm(\mu) = \pm\langle\mu, \left[\frac{\delta F}{\delta\mu}, \frac{\delta G}{\delta\mu}\right]\rangle. \tag{75}$$

Here $\mu \in \mathfrak{g}^*$, $[\xi, \mu]$ is the Lie bracket in $\mathfrak{g}$ and $\delta F/\delta\mu, \delta G/\delta\mu \in \mathfrak{g}$ are the functional derivatives of F and G.

Given a smooth Hamiltonian function $H : \mathfrak{g}^* \to \mathbb{R}$ on the Poisson manifold $(\mathfrak{g}^*, \{F,G\}_\pm(\mu))$, the time evolution of any smooth function $F : \mathfrak{g}^* \to \mathbb{R}$ is given by the abstract *Poisson evolution equation*

$$\dot{F} = \{F, H\}. \tag{76}$$

Now, the basis of Davydov's molecular model of *muscular contraction* (for general overview of muscular contraction physiology and mechanics, see [50, 55]) is oscillations of Amid I peptide groups with associated dipole electric momentum inside a spiral structure of myosin filament molecules (see [17–19]). There is a simultaneous resonant interaction and strain interaction generating a collective interaction directed along the axis of the spiral. The resonance excitation jumping from one peptide group to another can be represented as an exciton, the local molecule strain caused by the static effect of excitation as a phonon and the resultant collective interaction as a *soliton*.

Davydov's own model of muscular solitons was given by the *nonlinear Schrödinger equation* (NLS) [17, 18]

$$\mathrm{i}\psi_t = -\psi_{xx} + 2\chi|\psi|^2\psi \qquad (77)$$

for $-\infty < x < +\infty$. Here $\psi = \psi(x, t)$ is a smooth complex-valued wave function with initial condition $\psi(x, t)|_{t=0} = \psi(x)$ and χ is a nonlinear parameter. In the linear limit ($\chi = 0$) equation (77) becomes the standard Schrödinger equation for the wave ψ-function of the free 1D particle with mass $m = 1/2$ [18].

For a different (financial) application, with a variety of traveling-wave solutions of the NLS (77), including both sech- and tanh-solitons, solved in terms of Jacobi elliptic functions, see [56, 57] and references therein.

To put this muscular–contraction model into a rigorous geometrical settings, we can define the infinite-dimensional phase-space manifold $\mathcal{P} = \{(\psi, \bar{\psi}) \in S(\mathbb{R}, \mathbb{C})\}$, where $S(\mathbb{R}, \mathbb{C})$ is the Schwartz space of rapidly-decreasing complex-valued functions defined on $\mathbb{R}$). We define also the algebra $\chi(\mathcal{P})$ of observables on $\mathcal{P}$ consisting of real-analytic functional derivatives $\delta F/\delta\psi$, $\delta F/\delta\bar{\psi} \in S(\mathbb{R}, \mathbb{C})$. The Hamiltonian function $H\mathcal{P} \to \mathbb{R}$ is given by

$$H(\psi) = \int_{-\infty}^{+\infty} \left(|\psi_x|^2 + \chi|\psi|^4\right) \mathrm{d}x$$

and is equal to the total energy of the soliton, which is a conserved quantity for (77) (see, e.g. [99, 100]).

The Poisson bracket on $\chi(\mathcal{P})$ represents a direct generalization of the classical finite–dimensional Poisson bracket [49]

$$\{F, G\}_+(\psi) = \mathrm{i}\int_{-\infty}^{+\infty} \left(\frac{\delta F}{\delta\psi}\frac{\delta G}{\delta\bar{\psi}} - \frac{\delta F}{\delta\bar{\psi}}\frac{\delta G}{\delta\psi}\right) \mathrm{d}x. \qquad (78)$$

It manifestly exhibits skew–symmetry and satisfies Jacobi identity. The functional derivatives are given by

$$\delta F/\delta\psi = -\mathrm{i}\{F, \bar{\psi}\} \qquad \text{and} \qquad \delta F/\delta\bar{\psi} = \mathrm{i}\{F, \psi\}.$$

Therefore the algebra of observables $\chi(\mathcal{P})$ represents the Lie algebra and the Poisson bracket is the $(+)$ Lie–Poisson bracket $\{F, G\}_+(\psi)$. The nonlinear Schrödinger equation (77) for the solitary particle–wave is a Hamiltonian system on the Lie algebra $\chi(\mathcal{P})$ relative to the $(+)$ Lie–Poisson bracket $\{F, G\}_+(\psi)$ and Hamiltonian function $H(\psi)$. Therefore the Poisson manifold $(\chi(\mathcal{P}), \{F, G\}_+(\psi))$ is defined and the abstract Poisson evolution equation (76), rewritten here as $\dot{\psi} = \{\psi, H\}$, which holds for any smooth function $\psi\chi(\mathcal{P}) \to \mathbb{R}$, is equivalent to (77).

An alternative model of muscular soliton dynamics is provided by the *Korteweg–deVries equation* (KdV, see [49])

$$f_t - 6ff_x + f_{xxx} = 0, \qquad f_x = \partial_x f \qquad (79)$$

where $x \in \mathbb{R}$ and f is a real–valued smooth function defined on $\mathbb{R}$. This equation is related to the ordinary Schrödinger equation by the inverse scattering method (see [99, 100]). Note that the most common traveling-wave solutions of the KdV (79) are sech-solitons with the velocity c, of the form [105]

$$f(x, t) = \frac{c}{2} \mathrm{sech}^2 \left[\frac{\sqrt{c}}{2}(x - ct) \right].$$

We may define the infinite–dimensional phase–space manifold $\mathcal{V} = \{f \in S(\mathbb{R})\}$, where $S(\mathbb{R})$ is the Schwartz space of rapidly decreasing real–valued functions $\mathbb{R}$. Further, we define $\chi(\mathcal{V})$ to be the algebra of observables consisting of functional derivatives $\delta F/\delta f \in S(\mathbb{R})$. The Hamiltonian $H : \mathcal{V} \to \mathbb{R}$ is given by

$$H(f) = \int_{-\infty}^{+\infty} (f^3 + \frac{1}{2}f_x^2) \, \mathrm{d}x$$

and provides the total energy of the soliton, which is a conserved quantity for (79) (see [99, 100]).

As a real–valued analogue to (78), the $(+)$ Lie–Poisson bracket on $\chi(\mathcal{V})$ is given *via* (74) by

$$\{F, G\}_+(f) = \int_{-\infty}^{+\infty} \frac{\delta F}{\delta f} \frac{\mathrm{d}}{\mathrm{d}x} \frac{\delta G}{\delta f} \, \mathrm{d}x.$$

Again it possesses skew–symmetry and satisfies Jacobi identity. The functional derivatives are given by $\delta F/\delta f = \{F, f\}$. The KdV equation (79), describing the behavior of the muscular molecular soliton, is a Hamiltonian system on the Lie algebra $\chi(\mathcal{V})$ relative to the $(+)$ Lie–Poisson bracket $\{F, G\}_+(f)$ and the Hamiltonian function $H(f)$. Therefore, the Poisson manifold $(\chi(\mathcal{V}), \{F, G\}_+(f))$ is defined and the abstract Poisson evolution equation (76), rewritten here as $\dot{f} = \{f, H\}$, which holds for any smooth function $f : \chi(\mathcal{V}) \to \mathbb{R}$, is equivalent to (79).

Another alternative model of muscular soliton dynamics is provided by our SGE (1) $\phi_{tt} = \phi_{xx} - \sin\phi$. Again, we may define the infinite–dimensional phase–space manifold $\mathcal{V} = \{\phi \in S(\mathbb{R})\}$, where $S(\mathbb{R})$ is the Schwartz space of rapidly decreasing real–valued functions $\mathbb{R}$). Further, we define $\chi(\mathcal{V})$ to be the algebra of observables consisting of functional derivatives $\delta F/\delta\phi \in S(\mathbb{R})$. The Hamiltonian $H : \mathcal{V} \to \mathbb{R}$ is given by

$$H(\phi) = \int_{-\infty}^{\infty} \left[\frac{1}{2}(\pi^2 + \phi_x^2) + 1 - \cos\phi\right] \, \mathrm{d}x$$

and provides the total energy of the soliton, which is a conserved quantity for the SGE (1). The $(+)$ Lie–Poisson bracket on $\chi(\mathcal{V})$ is given *via* (74) by

$$\{F, G\}_+(\phi) = \int_{-\infty}^{\infty} \left(\frac{\delta F}{\delta\phi}\frac{\delta G}{\delta\pi} - \frac{\delta F}{\delta\pi}\frac{\delta G}{\delta\phi}\right) \mathrm{d}x.$$

Again it possesses skew–symmetry and satisfies Jacobi identity. The functional derivatives are given by $\delta F/\delta\phi = \{F, \phi\} \in S(\mathbb{R})$. The SGE (1), describing the behavior of the molecular muscular soliton, is a Hamiltonian system on the Lie algebra $\chi(\mathcal{V})$ relative to the $(+)$ Lie–Poisson bracket $\{F, G\}_+(\phi)$ and the Hamiltonian function $H(\phi)$. Therefore, the Poisson manifold $(\chi(\mathcal{V}), \{F, G\}_+(\phi))$ is defined and the abstract Poisson evolution equation (76), rewritten here as $\dot\phi = \{\phi, H\}$, which holds for any smooth function $\phi\chi : (\mathcal{V}) \to \mathbb{R}$, is equivalent to (1).

4. Conclusion

In this paper, we have reviewed sine–Gordon equation and its traveling wave solutions. These solitary spatiotemporal processes can serve as realistic models of nonlinear excitations in complex systems in physical sciences as well as in various living cellular structures, including intra–cellular ones (DNA, protein folding and microtubules) and inter–cellular ones (neural impulses and muscular contractions). We have showed that sine–Gordon solitons, kinks and breathers can give us new insights even in such long–time established and Nobel–Prize winning living systems as the Watson–Crick double helix DNA model and the Hodgkin–Huxley neural conduction model.

References

[1] Abdalla E., Maroufi B., Melgar B. and Sedra M., *Information Transport by Sine-Gordon Solitons in Microtubules,* Physica A **301** (2001) 169-173.

[2] Ablowitz M., Kaup D., Newell A. and Segur H., *Method for Solving the Sine-Gordon Equation,* Phys. Rev. Let. **30** (1973) 1262-1264.

[3] Ablowitz M. and Segur H., *Solitons and the Inverse Scattering Transform,* SIAM, Philadelphia 1981.

[4] Ablowitz M. and Clarkson P., *Solitons, Nonlinear Evolution Equations and Inverse Scattering,* Cambridge Univ. Press, Cambridge 1991.

[5] Abbott B., Hill A. and Howarth J., *The Positive and Negative Heat Production Associated with a Nerve Impulse,* Proc. R. Soc. London B **148** (1958) 149-87.

[6] Arnold V., *Geometrical Methods in the Theory of Ordinary Differential Equations,* Springer, Berlin 1983.

[7] Aubry S., *Breathers in Nonlinear Lattices Existence, Linear Stability and Quantization,* Physica D **103** (1997) 201-250.

[8] Bodo B., Morfu S., Marquié P. and Essimbi B., *Noise Induced Breather Generation in a Sine-Gordon Chain,* J. Stat. Mech. Theor. Exp. **01** (2009) 01026.

[9] Braun O. and Kivshar Yu., *The Frenkel-Kontorova Model,* Springer, New York 2004.

[10] Braun O. and Kivshar Yu., *Nonlinear Dynamics of the Frenkel-Kontorova Model,* Phys. Rep. **306** (1998) 1-108.

[11] Bullough R. and Caudrey P. (Eds.), *Solitons,* Springer, Berlin 1980.

[12] Caspi S. and Ben-Jacob E., *Toy Model Studies of Soliton Mediated Protein Folding and Conformation Changes,* Europhys. Lett. **47** (1999) 522-527.

[13] Chou K., Zhang C. and Maggiora G., *Solitary Wave Dynamics as a Mechanism for Explaining the Internal Motion During Microtubule Growth,* Biopolymers **34** (1994) 143-153.

[14] Darboux G., *Lecon sur la Théorie Géné rale des Surfaces* (3$^{\text{rd}}$ Edn), Chelsea, New York 1972.

[15] Das P. and Schwarz W., *Solitons in Cell Membranes,* Phys. Rev. E **51** (1995) 3588-3612.

[16] Dash P., *Correct Dynamics of Sine-Gordon 2π-Kink in Presence of Periodic Perturbing Force,* J. Phys. C Solid State Phys. **18** (1985) L125-L130 doi:10.1088/0022-3719/18/6/002.

[17] Davydov A., *The Theory of Contraction of Proteins Under Their Excitation,* J. Theor. Biol. **38** (1973) 559-569.

[18] Davydov A., *Biology and Quantum Mechanics,* Pergamon, New York 1982.

[19] Davydov A., *Solitons in Molecular Systems,* (2$^{\text{nd}}$ Edn), Kluwer, Dordrecht 1991.

[20] Derks, G., Doelman, A., van Gils S. and Susanto H., *Stability Analysis of π-Kinks in a 0-π Josephson Junction,* SIAM J. Appl. Dyn. Syst. **6** (2007) 99-141.

[21] Dodd R., Eilbeck J., Gibbon J. and Morris H., *Solitons and Nonlinear Wave Equations,* Academic Press, London 1982.

[22] Dustin P., *Microtubules,* Springer, Berlin 1984.

[23] Ellis J., Mavromatos N. and Nanopoulos D., *How Large are Dissipative Effects in Non-Critical Liouville String Theory?*, Phys. Rev. D **63** (2001) 024024.

[24] Ellis J., Mavromatos N. and Nanopoulos D., *String Theory Modifies Quantum Mechanics,* Phys. Lett. B **293** (1992) 37-48.

[25] Englander S., Kallenbach N., Heeger A., Krumhansl J. and Litwin S., *Nature of the Open State in Long Polynucleotide Double Helices Possibility of Soliton Excitations,* Proc. Natl. Acad. Sci. USA **77** (1980) 7222-7226.

[26] Faddeev L. and Takhtajan L., *Hamiltonian Methods in the Theory of Solitons,* Springer, Series Classics in Mathematics, Berlin 2007.

[27] FitzHugh R., *Mathematical Models of Threshold Phenomena in the Nerve Membrane,* Bull. Math. Biophys. **17** (1955) 257-269.

[28] Flach S., Miroshnichenko A. and Fistul M., *Wave Scattering by Discrete Breathers,* Chaos **13** (2003) 596-609.

[29] Flach S. and Gorbach A., *Discrete Breathers in Fermi-Pasta-Ulam Lattices,* Chaos **15** (2005) 015112.

[30] Flach S. and Gorbach A., *Discrete Breathers – Advances in Theory and Applications,* Phys. Rep. **467** (2008) 1-116.

[31] Flach S. and Gorbach A., *Discrete Breathers with Dissipation,* A Chapter in *Dissipative Solitons From Optics to Biology and Medicine,* A. Ankiewicz and N. Akhmediev (Eds), Lect. Notes in Physics **751** (2008) 1-32.

[32] Flach S. and Willis C., *Discrete Breathers,* Phys. Rep. **295** (1998) 182-264.

[33] Frenkel Y. and Kontorova T., On Theory of Plastic Deformation and Twinning. Phys. Z. Sowjetunion **13** (1938) 1-7.

[34] Fung Y., *Foundations of Solid Mechanics,* Prentice Hall, New Jersey 1965.

[35] Georgiev D., Papaioanou S. and Glazebrook J., *Solitonic Effects of the Local Electromagnetic Field on Neuronal Microtubules,* Neuroquantology **5** (2007) 276-291.

[36] Gonzalez J., Bellorin A. and Guerrero L., *How to Excite the Internal Modes of Sine-Gordon Solitons,* Chaos, Solitons & Fractals, **17** (2003) 907-919.

[37] Gonzalez J., Bellorin A. and Guerrero L., *Internal Modes of Sine-Gordon Solitons in the Presence of Spatiotemporal Perturbations,* Phys. Rev. E **65** (2002) 065601R.

[38] Gronbech-Jensen N. and Kivshar Yu., *Inverted Kinks in AC Driven Damped Sine-Gordon Chains,* Phys. Let. A **171** (1992) 338-343.

[39] Guilarte J., *Lectures on Quantum Sine-Gordon Models,* Univ. Fed. Matto Grosso, Brazil 2010.

[40] Gulevich D. and Kusmartsev F., *Perturbation Theory for Localized Solutions of Sine-Gordon Equation Decay of a Breather and Pinning by Microresistor,* Phys. Rev. B **74** (2006) 214303.

[41] Gulevich D., Kusmartsev F., Savel'ev S., Yampol'skii V. and Nori, F., *Shape Waves in 2D Josephson Junctions Exact Solutions and Time Dilation,* Phys. Rev. Lett. **101** (2008) 127002.

[42] Guo D., Wang Q. and Perc M., *Complex Synchronous Behavior in Interneuronal Networks with Delayed Inhibitory and Fast Electrical Synapses,* Phys. Rev. E **85** (2012) 061905.

[43] Heimburg T. and Jackson A., *On Soliton Propagation in Biomembranes and Nerves,* Proc. Natl. Acad. Sci. USA, **102** (2005) 9790-9795.

[44] Heimburg T. and Jackson A., *On the Action Potential as a Propagating Density Pulse and the Role of Anesthetics,* Biophys. Rev. Let. **2** (2007) 57-78.

[45] Haskins M. and Speight J., *Breathers in the Weakly Coupled Topological Discrete Sine-Gordon System,* Nonlinearity **11** (1998) 1651-1671.

[46] Hill A., *The Heat of Shortening and the Dynamic Constants of Muscle,* Proc. R. Soc. London B **76** (1938) 136-195.

[47] Hodgkin A. and Huxley A., *A Quantitative Description of Membrane Current and Application to Conduction and Excitation in Nerve,* J. Physiol. (London) **117** (1952) 500-544.

[48] Hodgkin A., *The Conduction of the Nervous Impulse,* Liverpool Univ. Press, Liverpool 1964.

[49] Ivancevic V. and Pearce C., *Poisson Manifolds in Generalised Hamiltonian Biomechanics,* Bull. Austral. Math. Soc. **64** (2001) 515-526.

[50] Ivancevic V. and Ivancevic T., *Natural Biodynamics,* World Scientific, Series Mathematical Biology, Singapore 2006.

[51] Ivancevic V. and Ivancevic T., *Geometrical Dynamics of Complex Systems*: *A Unified Modelling Approach to Physics Control Biomechanics Neurodynamics and Psycho-Socio-Economical Dynamics,* Springer, Dordrecht 2006.

[52] Ivancevic V. and Ivancevic T., *Applied Differential Geometry*: *A Modern Introduction,* World Scientific, Series Mathematics, Singapore 2007.

[53] Ivancevic V. and Ivancevic T., *Complex Nonlinearity Chaos, Phase Transitions, Topology Change and Path Integrals,* Springer, Series Understanding Complex Systems, Berlin 2008.

[54] Ivancevic V. and Ivancevic T., *Quantum Neural Computation,* Springer, Series Intelligent Systems, Control and Automation, Berlin 2009.

[55] Ivancevic V., *Nonlinear Complexity of Human Biodynamics Engine,* Nonlin. Dynamics **61** (2010) 123-139.

[56] Ivancevic V., *Adaptive-Wave Alternative for the Black-Scholes Option Pricing Model,* Cogn. Comput., **2** (2010) 17-30.

[57] Ivancevic V., *Adaptive Wave Models for Sophisticated Option Pricing,* J. Math. Finance **1** (2011) 41-49.

[58] Ivancevic V. and Ivancevic T., *Ricci Flow and Nonlinear Reaction-Diffusion Systems in Biology, Chemistry, and Physics,* Nonlin. Dynamics **65** (2011) 35-54.

[59] Ivancevic V. and Ivancevic T., *New Trends in Control Theory,* World Scientific, Series Stability, Vibration and Control of Systems, Singapore 2012.

[60] Ivancevic V. and Reid D., *Turbulence and Shock-Waves in Crowd Dynamics,* Nonlin. Dynamics **68** (2012) 285-304.

[61] Ivancevic T., Greenberg H. and Greenberg R., *Sport Without Injuries And Ultimate Health Through Nature, Science and Technology,* Springer, Series Cognitive Systems Monographs, Berlin (in press).

[62] Januar M., Sulaiman A. and Handoko L., *Nonlinear Conformation of Secondary Protein Folding,* Int. J. Mod. Phys. Conf. Ser. **9** (2012) 127-132.

[63] Kaup D. and Newell A., *Theory of Nonlinear Oscillating Dipolar Excitations in One-Dimensional Condensates,* Phys. Rev. B **18** (1978) 5162-5167.

[64] Kaup D., *Perturbation Theory for Solitons in Optical Fibers,* Phys. Rev. A **42** (1990) 5689-5694.

[65] Keener J. and McLaughlin D., *Solitons Under Perturbations,* Phys. Rev. A **16** (1977) 777-790.

[66] Khusnutdinova K. and Pelinovsky D., *On the Exchange of Energy in Coupled Klein Gordon Equations,* Wave Motion **38** (2003) 1-10.

[67] Kivshar Yu., Gronbech-Jensen N. and Samuelsen M., *Pi Kinks in a Parametrically Driven Sine-Gordon Chain,* Phys. Rev. B **45** (1992) 7789-7794.

[68] Kivshar Yu. and Malomed B., *Dynamics of Solitons in Nearly Integrable Systems,* Rev. Mod. Phys. **61** (1989) 763-915.

[69] Lal, P., *Kink Solitons and Friction,* Phys. Lett. A **111** (1985) 389-397.

[70] Lautrup B., Appali R., Jackson, A. and Heimburg T., *The Stability of Solitons in Biomembranes and Nerves,* Eur. Phys. J. E Soft Matter **34** (2011) 1-9.

[71] Lax P., *Integrals of Nonlinear Equations of Evolution and Solitary Waves,* Comm. Pure Appl. Math. **21** (1968) 467-490.

[72] Levi M., *Geometry and Physics of Averaging with Applications,* Physica D **132** (1999) 150-164.

[73] Lindblad G., *On the Generators of Quantum Dynamical Semigroups,* Comm. Math. Phys. **48** (1976) 119-130.

[74] Li Y., *Homoclinic Tubes and Chaos in Perturbed Sine-Gordon Equation,* Chaos, Solitons & Fractals **20** (2004) 791-798.

[75] Mavromatos N. and Nanopoulos D., *A Non-Critical String* (*Liouville*) *Approach to Brain Microtubules State Vector Reduction, Memory Coding and Capacity,* Int. J. Mod. Phys. B **11** (1997) 851-918 doi: 10.1142/S0217979297000460

[76] Marsden J. and Ratiu T., *Introduction to Mechanics and Symmetry A Basic Exposition of Classical Mechanical Systems* (2nd Edn), Springer, New York 1999.

[77] Mingaleev S., Gaididei Y., Christiansen P. and Kivshar Yu., *Nonlinearity-Induced Conformational Instability and Dynamics of Biopolymers,* Europhys. Lett. **59** (2002) 403-409.

[78] Miroshnichenko A., Flach S., Fistul M., Zolotaryuk Y. and Page J., *Breathers in Josephson Junction Ladders Resonances and Electromagnetic Wave Spectroscopy,* Phys. Rev. E **64** (2001) 066601.

[79] McLaughlin D. and Scott A., *Perturbation Analysis of Fluxon Dynamics,* Phys. Rev. A **18** (1978) 1652-1680.

[80] Meszena B., *System of Pendulums*: *A Realization of the Sine-Gordon Model,* Wolfram Demonstrations Project 2013.

[81] Nagumo J., Arimoto S. and Yoshizawa S., *An Active Pulse Transmission Line Simulating Nerve Axon,* Proc. IRE **50** (1962) 2061-2070.

[82] Newell A., *Solitons in Mathematics and Physics,* SIAM, Philadelphia 1985.

[83] Novikov S., Manakov S., Pitaevskii L. and Zakharov V., *Theory of Solitons*: *The Inverse Scattering Method,* Springer, Berlin 1984.

[84] Nanopoulos D., *As Time Goes By,* Riv. Nuovo Cim. **17** (1994) 1-53.

[85] Olsen O. and Samuelsen M., *Sine-Gordon 2π-Kink Dynamics in the Presence of Small Perturbations,* Phys. Rev. B **28** (1983) 210-217.

[86] Otwinowski M., Paul R. and Laidlaw W., *Exact Travelling Wave Solutions of a Class of Nonlinear Diffusion Equations by Reduction to a Quadrature,* Phys. Lett. A **128** (1988) 483-487.

[87] Perring J. and Skyrme T., *A Model Unified Field Equation,* Nucl. Phys. **31** (1962) 550-555.

[88] Polyanin A. and Zaitsev V., *Handbook of Nonlinear Partial Differential Equations,* Chapman & Hall/CRC Press, Boca Raton 2004.

[89] Pople J., *Molecular Association in Liquids II. A Theory of the Structure of Water,* Proc. Roy. Soc. London A **205** (1951) 163-178.

[90] Prilepsky J. and Kovalev A., *On the Internal Modes in Sine-Gordon Chain,* Phys. Rev. E **71** (2005) 046601.

[91] Rajaraman R., *Solitons and Instantons.* North-Holland, Amsterdam 1982.

[92] Salas A., *Exact Solutions of Coupled Sine-Gordon Equations,* Nonl. Anal. Real World Appl. **11** (2010) 3930-3935.

[93] Salerno M., *Discrete model for DNA-Promoter Dynamics,* Phys. Rev. A **44** (1991) 5292-5297.

[94] Salerno M., *Dynamical Properties of DNA Promoters,* Phys. Lett. A **167** (1992) 49-53.

[95] Salerno M. and Kivshar Yu., *DNA Promoters and Nonlinear Dynamics,* Phys. Lett. A **193** (1994) 263-266.

[96] Satarić M., Tuszyńsky J. and Zakula R., *Kinklike Excitations as an Energy-Transfer Mechanism in Microtubules,* Phys. Rev. E **48** (1993) 589-597.

[97] Satarić M., Zeković S., Tuszyńsky J. and Pokorni J., *Mossbauer Effect as a Possible Tool in Detecting Nonlinear Excitations in Microtubules,* Phys. Rev. E **58** (1998) 6333-6339.

[98] Satarić M. and Tuszyńsky J., *Relationship Between Ferroelectric Liquid Crystal and Nonlinear Dynamics of Microtubules,* Phys. Rev. E **67** (2003) 011901-011911.

[99] Seiler W. and Tucker R., *Involution and Constrained Dynamics I. The Dirac Approach,* J. Phys. A **28** (1995) 4431-4451.

[100] Seiler W., *Involution and Constrained Dynamics II. The Faddeev-Jackiw Approach*, J. Phys. A **28** (1995) 7315-7331.

[101] Sulaiman A., Zen F., Alatas H. and Handoko L., *Anharmonic Oscillation Effect on the Davydov-Scott Monomer in a Thermal Bath*, Phys. Rev. E **81** (2010) 061907.

[102] Tabor M., *Chaos and Integrability in Nonlinear Dynamics,* Wiley, New York 1989.

[103] Takeno S. and Peyrard M., *Nonlinear Modes in Coupled Rotator Models,* Physica D **92** (1996) 140-163.

[104] Temam R., *Infinite Dimensional Dynamical Systems in Mechanics and Physics* (2nd Edn), Springer, New York 1996.

[105] Terng C.-L. and Uhlenbeck K., *Geometry of Solitons,* Notices AMS **47** (2000) 17-25.

[106] Wikipedia, the free encyclopedia, *Sine-Gordon Equation,* 2012.

[107] Wolfram MathWorld, *Sine-Gordon Equation,* 2012.

[108] Yakushevich L., *Nonlinear Physics of DNA* (2nd Edn), Wiley, New York 2006.

[109] Yakushevich L., *The Effects of Damping, External Fields and Inhomogeneity on the Nonlinear Dynamics of Biopolymers,* Stud. Biophys. **121** (1987) 201-207.

[110] Yomosa S., *Soliton Excitations in Deoxyribonucleic Acid* (*DNA*) *Double Helices,* Phys. Rev. A **27** (1983) 2120-2125.

[111] Yomosa S., *Solitary Excitations in Deoxyribonuclei Acid* (*DNA*) *Double Helices,* Phys. Rev. A **30** (1984) 474-480.

[112] Zdravković S., Kavitha L., Satarić M., Zekovi ć S. and Petrović J., *Modified Extended Tanh-Function Method and Nonlinear Dynamics of Microtubules,* Chaos, Solitons & Fractals **45** (2012) 1378-1386.

[113] Zhang C.-T., *Soliton Excitations in Deoxyribonucleic Acid* (*DNA*) *Double Helices,* Phys. Rev. A **35** (1987) 886-891.

[114] Zharnitsky V., Mitkov I. and Levi M., *Parametrically Forced Sine-Gordon Equation and Domain Walls Dynamics in Ferromagnets,* Phys. Rev. B **57** (1998) 5033-5035.

[115] Zharnitsky V., Mitkov I. and Gronbech-Jensen N., *π Kinks in Strongly AC Driven Sine-Gordon Systems,* Phys. Rev. E **58** (1998) R52-R55.

Vladimir G. Ivancevic
Land Operations Division
Defence Science and
Technology Organisation
AUSTRALIA
E-mail address: Vladimir.Ivancevic@dsto.defence.gov.au

Tijana T. Ivancevic
Tesla Science Evolution Institute
Adelaide, AUSTRALIA
E-mail address: Tijana.Ivancevic@alumni.adelaide.edu.au